Page 7 is missing from the original thesis

QUASI-GEOSTROPHIC JET MEANDERING

by

DONALD ALBERT CAMPBELL

Sc.B., Brown University
(1972)

SUBMITTED IN PARTIAL FULFILLMENT
OF THE REQUIREMENTS FOR THE DEGREE OF
MASTER OF SCIENCE

at the

MASSACHUSETTS INSTITUTE OF TECHNOLOGY

August 1980

Signature of Author.....
Department of Meteorology
August, 1980

Certified by.....
Glenn Flierl
Thesis Supervisor

Accepted by.....
Peter H. Stone
Chairman, Departmental Committee on Graduate Students

Contents

QUASI-GEOSTROPHIC JET MEANDERING

by

DONALD ALBERT CAMPBELL

Submitted to the Department of Meteorology, August 1980, in partial fulfillment of the requirements for the degree of Master of Science.

ABSTRACT

The meandering of an oceanic jet such as the Gulf Stream is investigated. The flow is divided into three regions, one where the strong, non-locally generated jet dominates the flow, and two "far" regions that extend from where the jet profile goes to zero out to ∞. The vorticity equation in the far regions, on the f plane, reduces to the very nice $\nabla^2 p=0$. A set of coordinates is introduced called intrinsic coordinates that move and twist with the stream, for use in the analyses in the jet region. The vorticity equation is expressed in these coordinates and then scaled, taking advantage of the thinness of the jet and the dominance of the background flow in that region. The strong flow region is integrated over. The resulting equation has all terms except two expressed in terms of the position of the axis and its derivatives. These two are evaluated by matching them to information from the far field. Conversely, this integration across the stream can be viewed as including the dynamics from the stream region, to leading order, into a sort of matching condition for the pressures in the far regions. The process of getting the infomation from the far field entails the introduction of Greens formula techniques. The result is integral equations for the two terms at each time step. The solutions of these, in terms of the axis position, are plugged back into our vorticity equation to give a differential equation for the evolution of the axis position, which can the be stepped forward in time.

Section 4 contains the above program. Before doing that, an outline of some previous works on the Gulf Stream meandering is made in section 2. Appendix A sketches a vorticity development broad enough so these familiar models can be looked at in a uniform framework.

A minimum of standard results from a top-hat jet velocity profile (in appendix B the pressure jump conditions used in this type model are discussed at some length) are derived in section 3. They are used to discuss briefly some of the assumptions that go into our model, but primarily they are there to serve as a basis for a linear limit check of our model which we carry out in section 5.

Thesis Supervisor: Dr. Glenn Flierl
Title: Associate Professor of Oceanography

1. Introduction

An outstanding feature of the general ocean circulation is the strong currents that exist on the western boundaries of many basins, such as the Gulf Stream and the Kuroshio. The intensity of these currents has attracted the attention of seafarers from the time they were first encountered. Stommel (Reprint Edition, 1976, Chapter 1) has surveyed the written record on the Gulf Stream. By the 1800s observations were sophisticated enough to note the spatial shifting of the cold/warm fronts and of the high velocity region that constituted the jet. Today we call this process of shifting "meandering." Concomitant with the large relative increase in observations in the last few decades came an increase in attempts to build models that would demonstrate what the physics are that give rise to the meandering. The purpose of this work is to demonstrate that instability of an inertial jet can lead to meanders of the type we see in streams such as the Gulf Stream. The simplifications we make in this paper preclude trying to make a tight fit to oceanic data. The inclusion of some of those effects, particularly β, may be very difficult, and will be a subsequent project after we have established that the qualitatively right type of behavior can come out of such models. Our work will show that certain terms in the governing equation, and hence certain physical mechanisms, that have often been ignored (e.g., in the topographic steering models) can be very important and so must be included in any investigation.

The general ocean circulation problem, to fit the proper forcing and boundary conditions, requires one to consider the entire globe. We, however, will be looking locally at a jet. Hence we are assuming two things: first, that we can in some rough way include the effect of the

rest of the full problem, which here shows up as a posited background jet; and, second, that we can largely decouple the area of interest from the full problem, so the presence or absence of a meander in the jet does not cause radical changes in the flow far away or, in our model, in the posited jet. As background for our local approach that takes the jet as given we have reviewed in Section 2 some general ideas on why the open ocean jets we observe are there.

Section 3 uses the results from the simplest instability model to check assumptions and as a reference for section 5. As they are often referred to but seldom worked out in detail in the literature, the jump pressure conditions which go into this model have been worked out at length, both mathematically and physically, in Appendix B.

Robinson and Niiler (1967; RN) (papers that we will be citing often will have an abbreviation following the date,which will also appear in the bibliography) introduced an innovative coordinate transformation to facilitate studying the meanders at large amplitudes. As in our model below they posited a strong background jet with a given profile, constant in time and downstream. There they considered a steady balance, but that was extended by Robinson, Luyten, and Flierl (1975; RLF) to include time-dependent effects in the transformation. As their coordinates are necessarily somewhat messy and confusing and as we think they have potential for application to other finite amplitude problems such as internal waves, we spend time at the start of Section 4 developing them in greater depth than has been done previously in the literature.

RN applied their coordinate transformation to investigating the problem of topographical steering. We feel that the results of RLF lead to the possibility of the opposite conclusion, that the topographic steering is

not the dominant effect. The RLF model produced reasonable meandering even over a flat bottom. Our work here can be viewed as an extension, or correction, of that 1975 paper. Flierl and Robinson (to be published; FR) showed, and we redo in a simplified form in section 4B, that the scaling used in RLF was inconsistent. The proper scaling leads to a much more complicated problem, but one which we feel can exhibit the same type of plausible meandering behavior as found in RLF.

In Section 4C we introduce Green's formula techniques to solve the proper problem. We derive there the sought-for equation for the evolution of the jet axis.

We stress that this approach does not depend on the jet penetrating to the bottom or even to the deep ocean. This always has been a weak point in topographically steered models as Warren (1963) mentioned in his seminal work. Fuglister and Voorhis (1965) and recent work by Luyten (1977) and others suggest in fact that the deep flow below the Gulf Stream is not coupled tightly to the surface jet, making this investigation still more pertinent.

In the final section we look at the linear limit of our model and regain some of the well-respected traditional results of Section 3. This increases our confidence in the appropriateness of our method before we use it to go into the finite amplitude numerics in a future paper.

In this paper, where after setting up the governing equation we will only do out the analytically tractable linear limit, we will take periodicity in x similiar to the standard linear theory we will compare the results to. A fuller consideration of the boundary conditions, in line with the"inlet conditions " discussed in RLF, will be included in the subsequent paper

PAGES (S) MISSING FROM ORIGINAL

7

with the nonlinear results, where it is needed.

It is clear that the simplifications made in our model not only preclude a data fit as mentioned above, but also rule out explaining some aspects of the stream's behavior. With no inlet condition fixed in space, and on an f plane with no topography, there is no reason the stream should stay in one region of space as is observed. And we repeate that including all these effects, particularly the β effect, will not all be trivial. The major goal then of the model as it is, is to reproduce the large amplitude meandering found in RLF. The extensions which may entail significant changes in the mathematical method used here will be dealt with when needed.

2. Historical Building Blocks

The investigation in this paper into a possible meandering mechanism for a jet such as the Gulf Stream is seen as resting on thirty years of work on such problems. Here we will look briefly at some of the physics of earlier models. In particular, we will look at work on three aspects of the problem: 1) how the jet, which we will take as locally given, as discussed in the introduction, arises from basin-wide considerations; 2) why the current separates from the coast; and 3) what the inclusion of time dependence, key to our model, did in earlier attempts. All these papers were done with their own approach, their own notation. To facilitate comparison we have derived a general enough vorticity equation in Appendix A to see what is being stressed and what is being ignored in the models discussed here.

The first model created to explain why many oceans exhibit a strong western boundary current was put forward by Stommel (1948). It was a steady state, linear, homogenous fluid, flat bottom, lateral viscosity free model (from Appendix A: $\epsilon = \mathcal{E} = s = \alpha = 0$). He had an imposed stress at the top from the wind, and the bottom stress he parameterized as linearly related to the velocity, giving

$$\hat{\beta} v = -\gamma \sin \pi y + R(v_x - u_y) \quad \text{or} \quad R \nabla^2 p + \hat{\beta} p_x = \gamma \sin \pi y \qquad (2.1)$$

He solved it explicitly in a simple rectangular basin. The important physical result was that there were two regions, a thin one near the western shore and broad one over the rest of the basin where two different leading balances dominated (2.1). The change in planetary vorticity balanced the input stress ($\hat{\beta}$ and γ) over the basin (the famous Sverdrup, 1947, balance) while the change in planetary vorticity balanced the bottom

drag (β and R) in the jet region. Because such structure exists in the solution one could, as people did later and as a complicated basin geometry makes necessary, approach this by boundary layer techniques. A final comment on his model concerns the way the jet is caused non-locally but analyzed locally, as discussed above. The wind stress curl that drives the jet transfers its effects over the whole basin, but we can still look locally at the jet and determine the vorticity balance there. That the local and global problems can be separated, in this sense, is support for our approach below where we postulate the existence of a jet and look at it locally to determine its behavior.

Munk (1950) proceeded similarly, but kept $\alpha \neq 0$. Here the γ term again accounted for the input of vorticity at the surface but the stresses died off before reaching the bottom, so no $R\nabla^2 p$ bottom dissipation occurred. Rather the lateral viscosity gave the needed dissipation. His equation

$$(\alpha\nabla^4 - \beta\partial_x)p = \gamma(\tau_y^{(x)} - \tau_x^{(y)}) \qquad (2.2)$$

also exhibited a boundary layer type solution. The interior had the same Sverdrup balance as Stommel had, while the balance in the jet was between the advection of the planetary vorticity gradient β and the dissipation $\alpha\nabla^4 p$. He put in realistic data from the Pacific and generated oceanic gyres that bore some resemblance to the real gyres. The value he used of $A_H = 5 \times 10^7$ cm^2/sec gave what he then thought was an appropriate Gulf Stream width of somewhat over 200 km.

A triangular basin was introduced in Munk and Carrier (1950) (and they therefore used the boundary layer approach) leading to two improvements.

First, the gyres more strongly resembled the observed gyres than in the square basin model. And second, a given value for A_H gave a thinner jet, a problem we will now take up in relation to the next type of model that came along.

It was soon realized that a more realistic width of the jet was 50 km. This corresponded to a much lower A_H. Even in the triangular basin where the thinner jet corresponded to a higher A_H than in the square basin, the needed A_H was so low that an internal inconsistency arose. Since the ignored inertial terms became larger than the retained frictional terms in the boundary layer, people began to look at the inertial terms. These terms will be in the model built in this paper. Further, they play a key role in our preferred explanation for the jet separation, described below, part of the background for our postulated open ocean jet that we investigate.

As Morgan (1956) pointed out, given the input of vorticity by the wind there must be some region where its dissipation is important. But the first inertial model sidestepped this by ignoring forcing. Keep in mind that because the equation is nonlinear the resulting solutions cannot even be viewed as useful in solving the forced problem for given boundary conditions in the way such solutions are used in linear theory. Fofonoff (1954), in his approach, used both the Bernoulli and vorticity equations, but for quasigeostrophic dynamics the Bernoulli equation is superfluous. His physics included taking $\epsilon = \alpha = \gamma\ (= R) = 0$ and thus getting

$$J(\psi, \varepsilon \nabla^2 \psi + 1 + \beta \hat{y}) = 0 \quad \text{or} \quad \nabla^2 \psi + \frac{1}{\varepsilon} \cdot \frac{\beta}{\varepsilon} y = F(\psi) \qquad (2.3)$$

for some function F. Taking a particularly simple form of F, he generated a solution with both eastern and western boundary currents, and a north, south, or inbetween latitudinal current. It did not resemble the observed ocean flow, suggesting, as expected, that the whole basin was not dominated by an inertial balance. But parts of the basin still might well be so dominated, as looked at in the next models.

Charney (1955) accepted a Sverdrup interior as a given and looked at the jet under the assumption that the inertial terms dominated the viscous terms there (as mentioned, viscous terms must enter somewhere, of course, but he didn't investigate those regions). He worked with a two-layer model, with the bottom layer quiescent (see Stern, 1961, for what this means physically) and observed that his model could cause the jet to separate from the coast to conserve its potential vorticity. To within appropriate approximations, equation A.13 can be rewritten here, for $\gamma = R = \alpha = 0$,

$$\left(\frac{\epsilon}{\hat{\epsilon}}\partial_t + u\partial_x + v\partial_y\right)\left(\frac{\epsilon(v_x - u_y) + 1 + \beta y}{1 - sh}\right) = 0 \qquad (2.4)$$

or dimensionally

$$\left(\partial_t + u\partial_x + v\partial_y\right)\left(\frac{\mathcal{J} + f}{h}\right) = 0$$

Stommel (1955, 1976, p. 109) used a simplification of this in a quick look at one transect of the Gulf Stream. He assumed potential vorticity constant everywhere, not just along stream lines as required by the above equation. He calculated v from this and compared it to v computed hydrographically. Except at the inner edge of the stream he got a reasonable match supporting the idea that the inertial terms do dominate the frictional

terms there, and that they should be important in our model.

We will now look at three ideas on why the jet separates from the coast. We will also use the first model as a jumping off place for a discussion on the effects of viscosity even when inertial terms dominate, something that is relevant to our model below where we assume on the first pass that friction can be ignored. The second model was really created to look at the stream path over the continental rise, but the implication of β and topographic steering is that it must also control separation.

Ignoring viscosity until some post-facto considerations Carrier and Robinson (1962) built an inertial model and were able to get the jet to separate from the western boundary at the maximum of the wind stress curl. Their two-gyre ocean with strong jets on the northeast besides southwest walls, and the nature of their central jet, did not correspond very well to reality. There were internal inconsistencies too. For example, Section 5, which tries to fix up the viscosity problem, has stream lines that nowhere go through a viscosity region. So we reject this as the cause of separation. We will shortly discuss a little about some recent numerical models which also have seperation resulting from the wind pattern imposed, though there it is a two gyre wind. The models have some results we like, so we will argue why those results should equally well follow using a different seperation mechanism, and continue not to believe in wind caused seperation.

A second explanation for separation is associated with Warren (1963). His paper tried to show that the meanders of the Gulf Stream (and hence, in passing, the separation) are determined by topographic steering. Stommel (1976, p. 11) cites earlier work on this by Eckman, Sverdrup et al., and Neuman. In the 1940s the meteorologists advanced the formulation of the problem considerably, especially Rossby (1940), Charney and Eliassen (1949) and Bolin (1950). The Japanese school of oceanography applied this method in the 1950s, for example Fukuoka(1957)

But Warren's work is often taken as seminal, as it attempted to be more quantitative than those before and to check the theory with data. However there were many problems with the method he developed. He ignored the $\partial S/\partial t$ term, which we will see below can be important, after conceeding it was hard to estimate its size. Hansen (1970) looked at the adequacy of this exclusion and concluded that it might all right for describing the mean Gulf Stream, but certainly not the meanders. Bringing in the effects of the bottom topography in a simple way is difficult. His results were shown by Robinson (1971) to be critically sensitive to the spatial averaging scheme he used for the depth. And further there is the problem he brought up in his paper and which we mentioned in the introduction: what if the bottom flow is not parallel to the main jet flow? Although Schmitz, Robinson, and Fuglister (1970) felt they generally had coherence with some exceptions (which become problems for the theory whenever they occur, as they should change the steering), later works by Robinson, Taft, and Schmitz (1973) and Luyten (1977) suggest even less linkage of the bottom flow to the jet. And finally his method assumes that the change in angle of his inlet is so slow relative to the propagation downstream

of fluid particles that the stream one sees in the ocean can be taken as everywhere having the potential vorticity it has at the inlet. In fact, of course, particles a distance vt downstream where v is the particle velocity, would have the potential velocity the inlet had time t ago, if potential vorticity is conserved.

We feel that the most reasonable explanation for separation was put forward by Parsons (1969), working roughly from equation (2.4) above, for a two-layer model. The usual north Atlantic type wind forcing causes a western boundary jet in the top layer. But this is accompanied by a shoaling of the interface as one goes north in this current. For a given amount of warm water and a given strength of forcing, the depth of the top layer at the west wall will at some point go to zero. Stronger forcing or less warm water moves that point south, and conversely. The current beyond that cannot stay on the west wall, and is forced to enter the open ocean. Kamenkovitch and Reznik (1972) worked out some messy mathematical loose ends to the theory, and incidentally got a countercurrent under the Gulf Stream, showing the flexibility of this method versus the topographic steering approach. Veronis (1973) used this type of two-layer model with separation to build a model for the entire world ocean, getting surprisingly good results. In a less transparent way the gigantic ocean-atmosphere model reported on by Bryan, Manabe and Pacanowski (1975) and the earlier and cruder model by Takano (1975) had separation caused by the surfacing of the sharp stratification front, as above, but where now the stratification was not an input as in the two-layer model but also an output of the model. More support for this type of separation model came from Golan (1979) who used Parson's model to look at the heat exchange between the ocean and atmosphere and got a reasonable fit to data.

Finally, we will look at some early works that included the time-dependent terms and looked-for instabilities. Haurwitz and Panofsky (1950) first introduced the idea that the meanders resulted from an instability of the velocity profile. They looked at the linearized frictionless vorticity equation for normal mode motion and straight line background profiles, as we will do for one such case in Section 3. Two results of interest they found which we should keep in mind are: first, as Rayleigh (1883) showed, the broader the transition zone from the central jet velocity to the surrounding quiescent ocean, the less unstable the profile is; and second, moving the jet near the shore tends to stabilize it.

In a paper by Lipps (1963) an attempt was made to get a dominant e-folding rate and wavelength for the Gulf Stream from instability theory. He chose a particular profile that he could deal with analytically. Drazin and Howard (1966) showed that such results are sensitive to the choice of profile. Our method below will depend on integrals of the background profile, much less sensitive parameters, ones that perhaps we can somewhat more meaningfully measure. The top-hat model we will look at can also be viewed as depending on integrated parameters, as was discussed and used at length by Flierl (1976). Finally, there is again the problem that underlies all results from linear theory: there is no real reason to think they should describe the finite amplitude meanders we really see. This problem of course is the motivation for our work, and will not appear in our nonlinear formulation.

The RLF (1975) paper is the direct antecedent of our work. It followed a series of papers by Robinson and various co-workers which began in 1965. The unusual coordinate system used in RLF and by us was introduced by RN (1967) in a work which tried to formalize better, so they could be

better evaluated, Warren's ideas on bottom steering. We feel especially that the results of RLF support the anti-bottom steering advocates. In their model they generated a meandering path without any bottom topography, that is, they showed that the time-dependent terms are capable of producing the qualitatively correct type of behavior. As we will show below there were inconsistencies in the formulation of that work and the correctly posed mathematical problem unfortunately becomes much more difficult. A goal of our work will be to show that one can still get meandering from the correctly posed problem without relying on bottom topography, particularly important in view of the question of the nature of the deep flow below the stream as mentioned above.

We want to briefly touch on a very important recent approach to this time dependent instability problem, that of numerical modeling. Once he gets his jet off the north wall, Holland(1978) gets very intresting meandering and even ring-like shedding by his stream. His pictures also give some support to our assumption of a uniform downstream structure of the jet. We note he gets seperation by driving it with a two gyre wind, but we believe that, as he points out, the important point is that the jet is no longer supported by the wall, and similar behavior would hold for seperation caused by the density field. It would be worthwhile to do a stability analyses of such experements in the spirit of Haidvogel and Holland(1978), using our formulation below.

3. The Standard Linear Problem

We are interested in looking at the validity of some of the simplifications that will be built into our model below. To do that we will introduce what we call the Standard Linear Problem with a top-hat background flow profile. We will develop the model only to the extent needed to make some observations about our simplifications, and readers interested in the model itself should look at the fuller examination in Flierl (1976). We, of course, are not guaranteed anything about the finite amplitude behavior by the linear behavior, but we will take evidence of the reasonableness of our simplifications in the infinitesimal limit to be suggestive of reasonableness in general. We will also use this model to make some comments on parts of the methodology we will be using below. We will develop the model first, and then go on to the comments.

By the top-hat model we refer to an unperturbed state that is a zonal jet

$$U^*(y^*) = \begin{cases} 0 & \text{if } |y^*| > \ell^* \\ U_0^* & \text{for } |y^*| < \ell^* \end{cases} \triangleq U_0^* U(y)$$

where $y \triangleq y^*/\ell^*$.

Our governing equation will be

$$\left(a\frac{\partial}{\partial t} - P_y\frac{\partial}{\partial x} + P_x\frac{\partial}{\partial y} \right)\left(\nabla^2 P + \frac{\hat{\beta}}{E} y \right) = 0 \qquad (3.1)$$

which is just our vorticity equation A.14 with the following modifications: first, in addition to its being homogeneous, we have taken it flat bottomed (s = 0) and frictionless (R = α = ν_4 = 0). We have called $\frac{\beta^*}{\varepsilon} \triangleq a$, where a represents the different scaling c^* and U_0^* might have, that is, $c^* = a\, U_0^*\, c$. While keeping the x* scale L* (we will indicate how this

is determined below) as in the appendix, we now no longer take the y* scale the same, but rather scale it by l^*, the half width of the stream, 25 km. We are interested in how the $P_{x^*}^* \sigma^*$ term compares to the other terms, all of which have U_o^* in them. This suggests looking at the length scale $\sqrt{U_o^*/\beta^*}$. Defining $\tilde{\beta} = \beta^* L^{*2}/U_o^*$ we get an O(1) $\tilde{\beta}$ for any $(L^*)^2 \approx U_o^*/\beta^*$. We will see below $k_o^{*2} = \beta^*/U_o^*$ is a cut off for unstable waves, so we will define $(L^*)^{-2} \triangleq k_o^{*2} = \beta^*/U_o^*$. Hence $\tilde{\beta} \equiv 1$, but we will usually carry it as $\tilde{\beta}$ to keep track of which terms arise from the gradient of the planetary vorticity. This will be our x* scale. With $\beta^* = 2 \times 10^{-13}$ 1/cm-sec and $U_o^* = 30$ cm/sec, L* = 150 km. Note L* is not a wave length, since $(L^*)^{-1} = k^*$; rather, it corresponds to a wavelength $L^*_{w.L.} = 2\pi \times 150$ km. This is a little longer than what observations indicate the dominant wavelength in the meanders are (see, e.g., Hansen (1970), who comes up with a length of 320 km as observed), but as an upper cut off that is reasonable. We will call $\ell^*/L^* \triangleq \lambda = .167$

If we recall that the p's in (3.1) are total p_T's, and we relabel $-(P_T)_y = U_{yy} - r P_y$ and $(P_T)_x = r P_x$ where the non-subscripted p's now represent the perturbation pressure and the nondimensional r allows them to be a different scale than the O(1) background flow, (3.1) becomes (recalling $U_y = U_{yy} = 0$ in all regions)

$$\left(a\frac{\partial}{\partial t} + U\frac{\partial}{\partial x}\right)\left(P_{yy} + \lambda^2 P_{xx}\right) + P_x \lambda^2 \beta = 0 \qquad (3.2)$$

The usual substitution $p(x,y,t) = p(y) e^{ik(x-ct)}$ then gives us

$$(U - ac)\left(P_{yy} - \lambda^2 k^2 p\right) + p\lambda^2\beta = 0 \qquad (3.3)$$

First we will show that for any symmetric jet any solution to (3.3) can be thought of as the sum of an even solution, called a sinuous or

firehose mode, and an odd solution, called a varicose or sausage mode. For an even v the operator in (3.3), written as $\mathcal{L}_+[p(y)] = 0$, is even. The "+" indicates that the dummy variable is +y. We will change the dummy +y to -y in both $\mathcal{L}_+$ and p(y) to get $\mathcal{L}_-[p(-y)] = 0$. But, since the operator is even, $\mathcal{L}_+ = \mathcal{L}_-$. Hence, $\mathcal{L}_+[p(-y)] = 0$ which says that if p(y) is a solution so is p(-y). Since $\mathcal{L}_+$ is linear the even function $E(y) = .5\,(p(y) + p(-y))$ and the odd function $O(y) = .5\,(p(y) - p(-y))$ are also solutions. So any solution p(y) can be thought of as composed of even and odd parts, p(y) = E(y) + O(y). Given that the Gulf Stream is more or less sinuous, we will restrict ourselves to looking at firehose modes.

Because we are looking at even modes we need only use the matching conditions at y = 1 and the condition at $+\infty$, and add a condition at y = 0, $p_y(0) = 0$, instead of also using the conditions at y = -1 and $y = -\infty$.

Equation (3.3) can be explicitly written

$$(1 - ac)(p_{yy} - \lambda^2 k^2 p) + p\lambda^2\beta = 0 \tag{3.4}$$

in the jet and

$$(-ac)(p_{yy} - \lambda^2 k^2 p) + p\lambda^2\beta = 0 \tag{3.5}$$

outside. Now provided $ac \neq 0$ or 1, which can be verified at the end, we can write these over in a more standard form (see Figure 3.1 for the regions) and solve them.

$$p_{yy} - \lambda^2(k^2 - \beta/(1-ac))p = 0 \Rightarrow p_{II} = B\cosh \lambda\mu_2 y \tag{3.6}$$

(Region II, inside the jet)

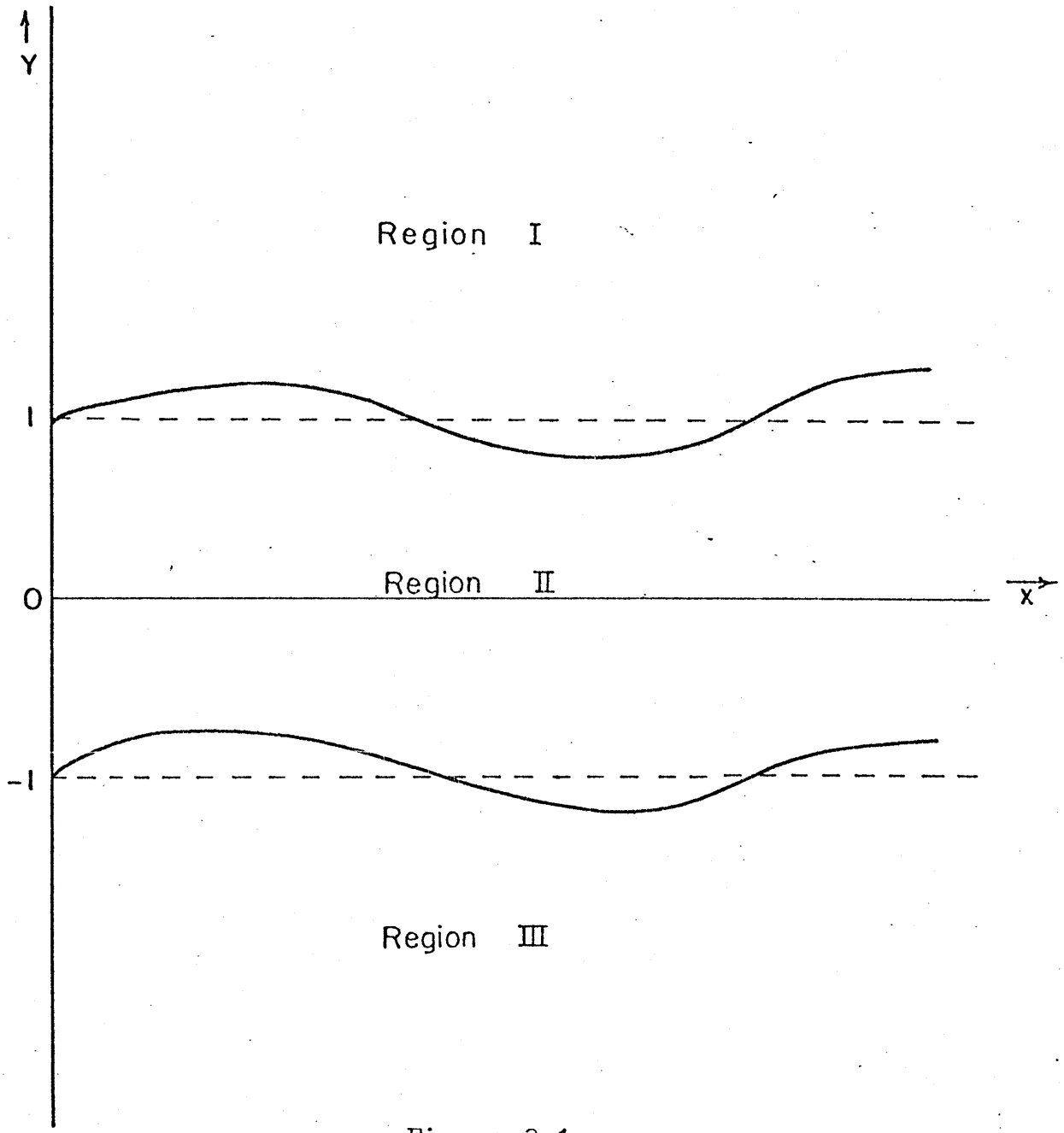

Figure 3.1

$$P_{yy} - \lambda^2 (k^2 + \beta/ac) p = 0 \Rightarrow P_I = A e^{-\lambda \mu_1 y} \tag{3.7}$$

(Region I, outside the jet)

where we have used the conditions at $+\infty$ and 0 to get these forms. We will call $\mu_1 \equiv \sqrt{k^2 + \beta/ac}$ and $\mu_2 = \sqrt{k^2 - \beta/1-ac}$. The cosh in P_{II} is understood to take complex arguments where appropriate. Since it is a homogeneous problem, there will be an arbitrary multiplicative constant in the final solution. We normalize by setting A = 1. Applying the two matching conditions from the appendix

$$\frac{P_I}{-ac} - \frac{P_{II}}{1-ac} = 0 \quad \text{at } y = 1 \tag{B.7}$$

and

$$-ac(P_I)_y - (1-ac)(P_{II})_y = 0 \tag{B.9}$$

give respectively

$$\frac{e^{-\lambda \mu_1}}{-ac} = \frac{B \cosh \lambda \mu_2}{1-ac} \tag{3.8}$$

and

$$ac \lambda \mu_1 e^{-\lambda \mu_1} = B(1-ac) \lambda \mu_2 \sinh \lambda \mu_2 \tag{3.9}$$

Eliminating B gives the dispersion relation for c

$$(1-ac)^2 \tanh \lambda \sqrt{k^2 - \beta/1-ac} = \frac{-\sqrt{k^2 + \beta/ac}}{\sqrt{k^2 - \beta/1-ac}} (ac)^2 \tag{3.10}$$

Solving for B gives

$$B = -\frac{e^{-\lambda \mu_1}}{ac} \frac{(1-ac)}{\cosh \lambda \mu_2} \tag{3.11}$$

Note that for $c \ll 0(1)$ this gives $B \gg 0(1)$.

Before beginning our discussion we want to consider when the $\tanh \lambda \mu_2$ in (3.10) can be replaced by a simple approximation. As $k \to 0$ this goes to $\tanh i\lambda = i \tan \lambda \approx i\lambda$ for $\lambda = .167$ (noting $\beta/(1-ac^2)$). On the other hand, when $\mu_2 = 10$, from $k \approx 10$, $\tanh 1.67 = .93$, and for $\mu_2 = 20$, $\tanh 3.34 = .99$, so from there to $k = \infty$ we can replace $\tanh \lambda\mu$ by 1. Recalling that we are not after details, we will make use of both approximations where appropriate below.

We will now look at four subsections on

A) our main use for the linear results

B) support for the "parallel jet" approximation below

C) support for using an f plane

D) support for our integrate-across-the-stream approach

A) The central reason for working out and including these standard results is to provide a basis for a comparison for our model below. In Section 5 we will take the linear limit of our fully nonlinear model in Section 4 and show that we can get a dispersion relation corresponding to (3.10). Having this in mind, we could proceed right to the development in Section 4. But we want to pause also to use this model, where we can see how certain changes affect the results, to support a few parts of Section 4.

B) One of the approximations we build into our model is that there exists a strong jet that stays parallel to its own axis as that axis meanders. This can of course be motivated by what we see in the ocean. But we can get further motivation by looking at the results of this linear theory. Figure 3.2a shows how parallel the flow stays as one goes to a

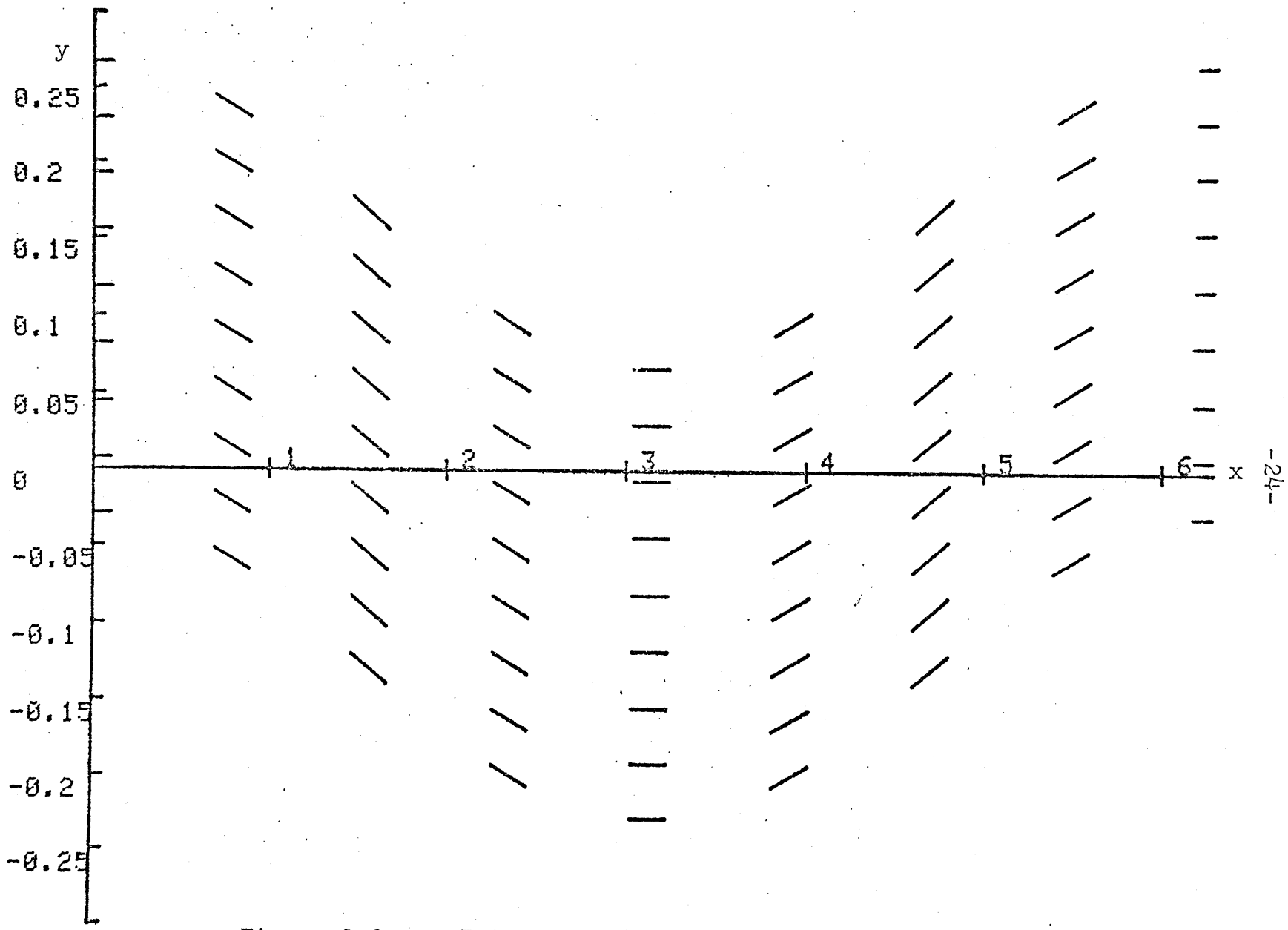

Figure 3.2a Total velocity vectors at varios x and y positions in the interior. Note the extreme parallelism between what are the most non parallel parts, the edge and the center. The ordinate is magnified.

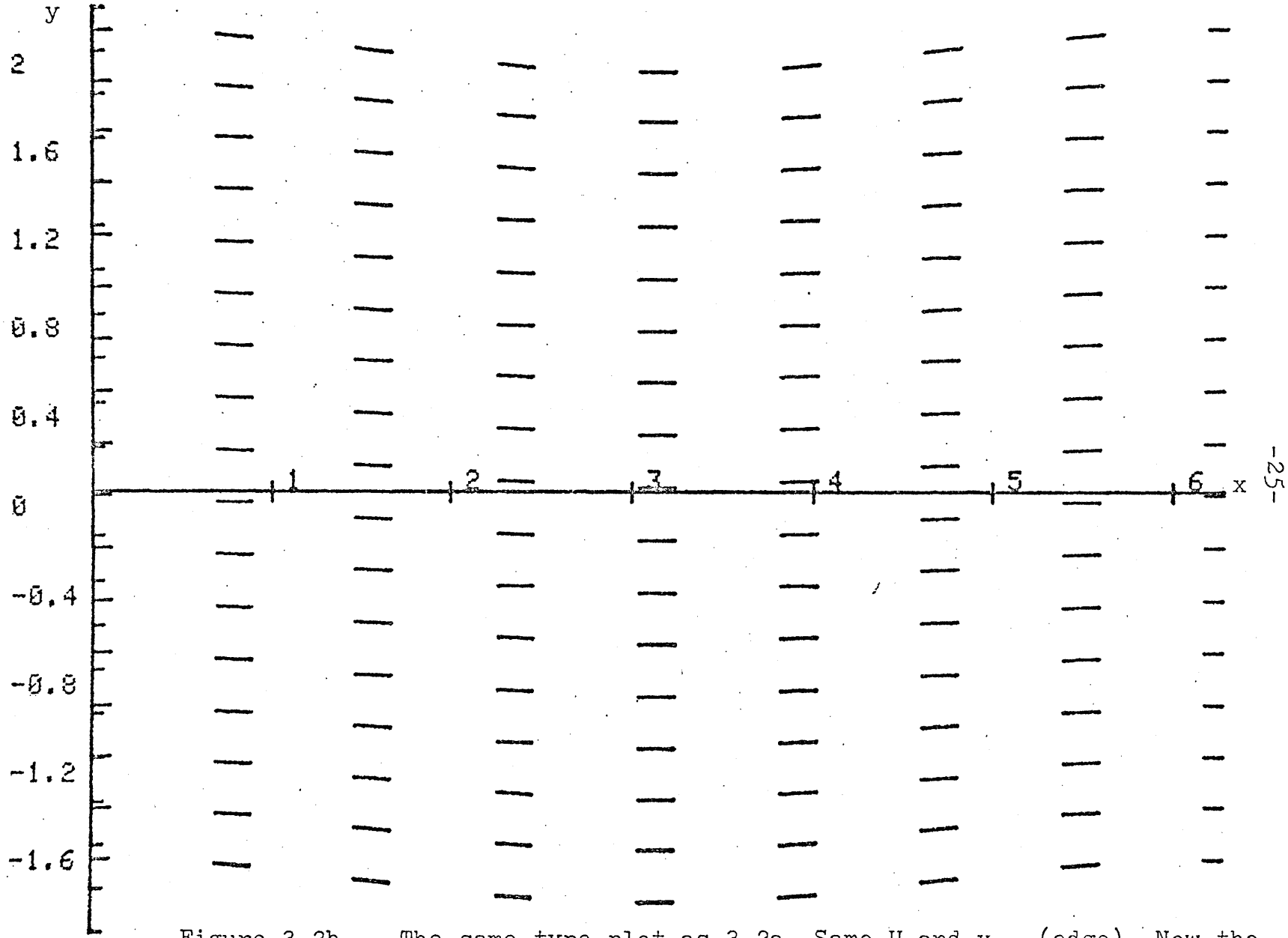

Figure 3.2b The same type plot as 3.2a. Same U and v_{max}(edge). Now the jet is wider and the y scale is changed. By looking at the biggest contrast, the edge to the middle at $\pi/2$ we see this is not everywhere so parallel as in 3.2a.

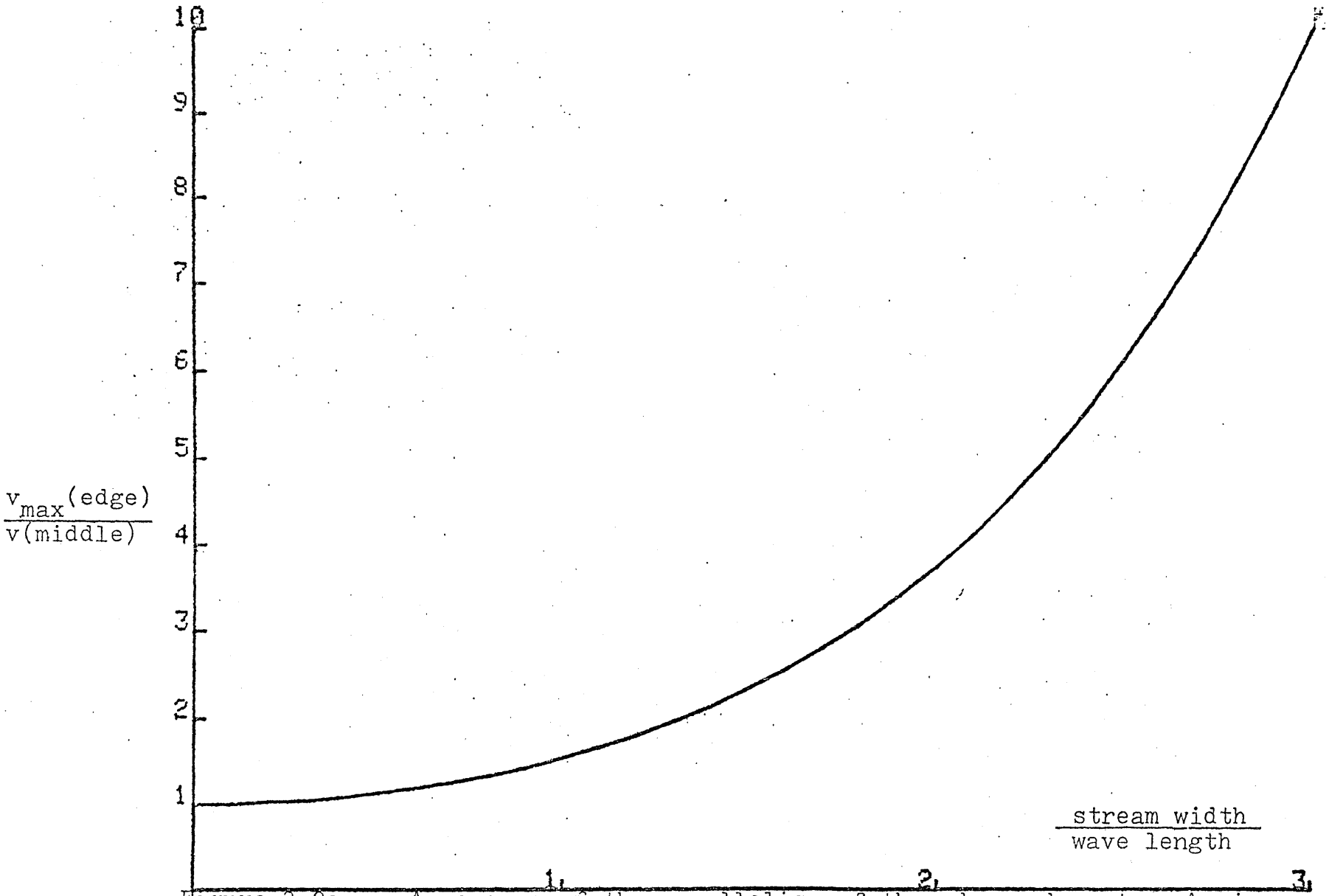

Figure 3.2c A measure of the parallelism of the edge and center. As in a and b, U is 1 throughout the jet and the maximum v(edge) is .1. Hence this is the ratio at the least parallel place, $x=\pi/2$ in 3.2a,b, since $\sin\pi/2=1$. The abscissa on this for a would be $.34/2\pi, 4/2\pi$ for b.

"finite" amplitude, but an amplitude still small enough so the nonlinear terms are negligible. The point is that for the corresponding varicose mode a strong parallel jet approximation clearly would not be appropriate. But even for the even mode, Figure 3.2b shows that this approximation is tied to the thinness of the jet. In Figure 3.2c we have graphed a measure of the deviation from parallelism for such cases as in Figures 3.2a,b, again showing the appropriateness of the strong parallel jet approximation for the thin jet.

C) Although we carry β in much of the development of Section 4, for use in subsequent works, this work will look at $\beta = 0$, at the f plane. We can examine what effect the presence of β has in this model. In the limit $\beta = 0$ (3.10) becomes (or the following could be derived from the basic equations with $\beta = 0$)

$$(1-ac)^2 \tanh \lambda k = -(ac)^2 \tag{3.12}$$

Figure 3.3a is a graph of (3.12). Note as $k \to \infty$ our approximation tanh $\to 1$ holds and we get $ac = \frac{1}{2} \pm i\frac{1}{2}$. We see that all very short waves have this maximum growth rate, that no preferred wave emerges. We will see below that this still holds for $\beta \neq 0$.

For $\beta \neq 0$ it simplifies things a lot to use the approximations discussed above for tanh. In Figure 3.3b we show how well replacing tanh x by x reproduces the long wave section of Figure 3.3a, while giving a false maximum ac_i in the short wave region. Keeping in mind that the short wave region will be unreliable, we reduce (3.10) to

$$(1-ac)^2 \lambda \left(k^2 - \beta/1-ac\right) = -\sqrt{k^2 + \beta/ac}\,(ac)^2 \tag{3.13}$$

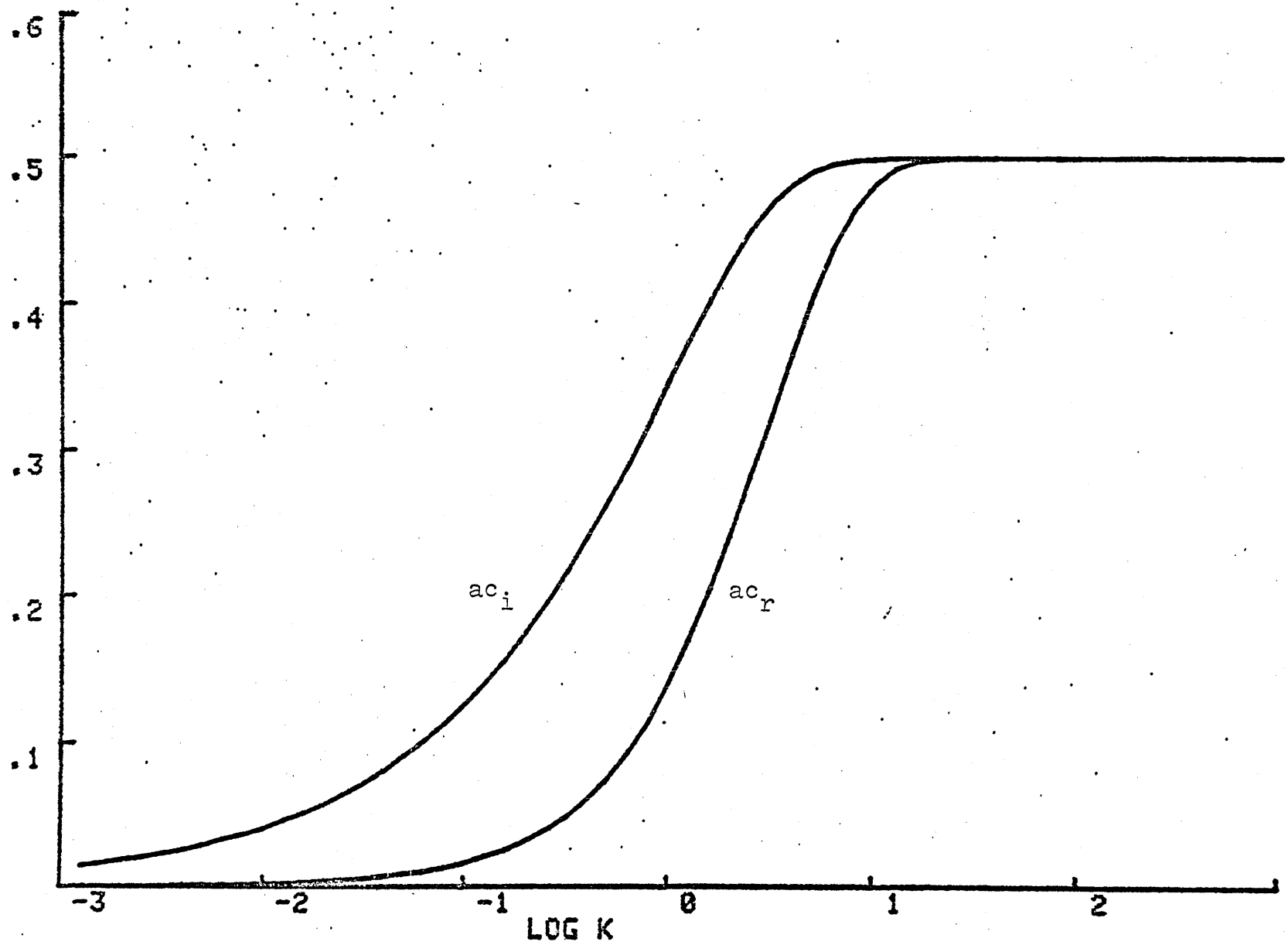

Figure 3.3a

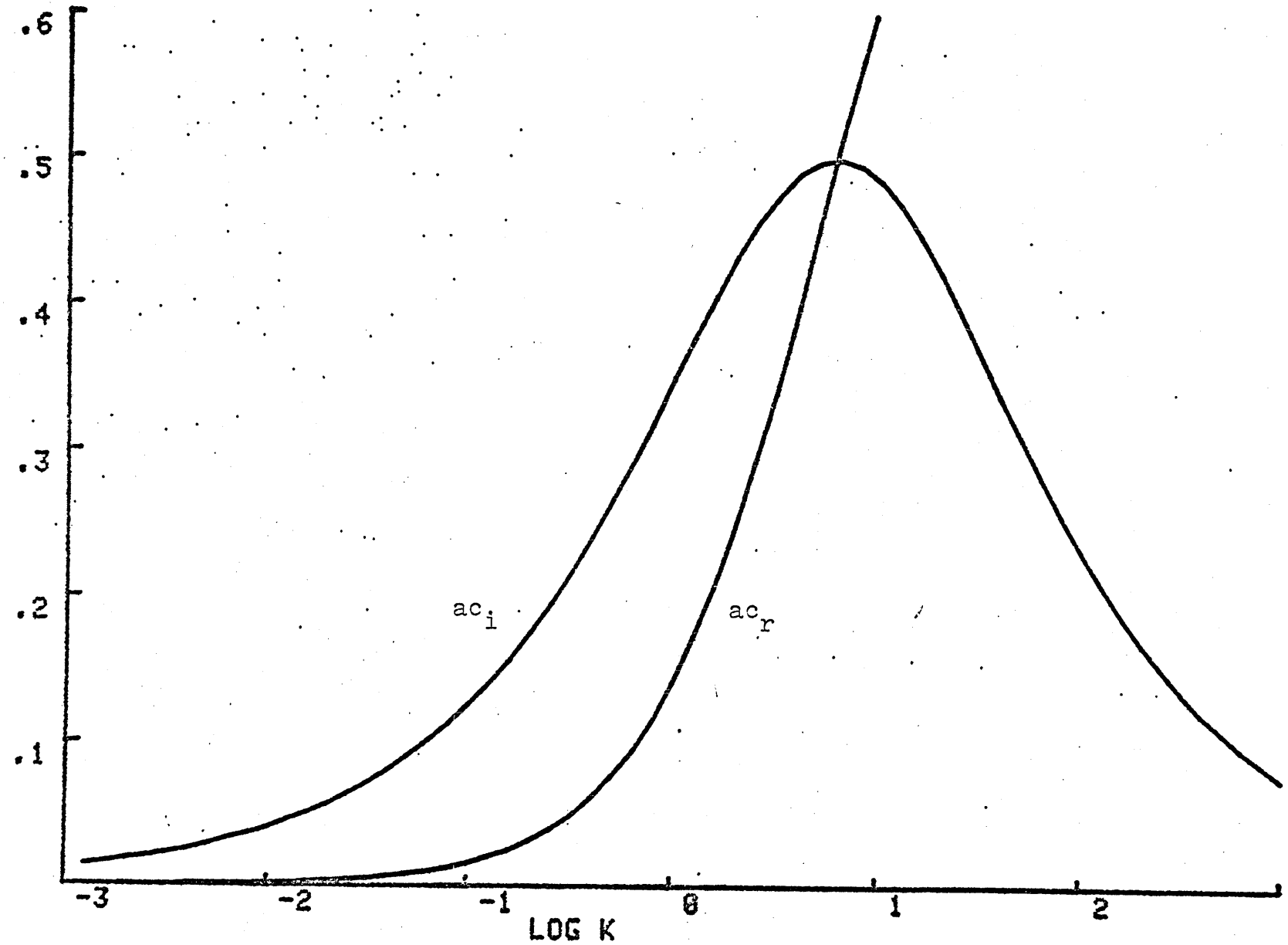

Figure 3.3b

which is graphed in Figure 3.4 . The striking difference from the $\beta = 0$ case is that now we have a long wave instability cut off. But although this at first seems qualitatively unrelated to the $\beta = 0$ case, Figures 3.5a and 3.5b for $\beta = .1$ and $\beta = .01$ respectively show in what way one approaches the $\beta = 0$ limit continuously. The cut-off point is seen to be marching off to $k = \infty$ as $\beta \to 0$. So the exclusion of β just changes the long waves from stable to weakly, slowly growing. As the short waves are seen to grow faster and so linearly dominate, we can consider this difference not to be crucial, and we will now look at the short waves. We would like to find a fastest growing wave, to suggest a possible length scale we might find, keeping in mind that quasi-linear theory (Pedlosky, unpublished) makes clear this need not in all cases be the wave that grows to maximum amplitude at finite amplitude. We replace tanh by 1 as discussed above to get

$$(1-ac)^2\left(k^2-\frac{\beta}{1-ac}\right)^{1/2} = -\left(k^2+\frac{\beta}{ac}\right)^{1/2}(ac)^2 \qquad (3.14)$$

Figure 3.6 shows we again get the limit $ac = \frac{1}{2} \pm i\frac{1}{2}$, as can be easily verified analytically, and as is expected physically since the β effect gets swamped as we go to the $\beta = 0$ results. Again we do not get a preferred wave.

So we have seen that with or without β the top-hat model gives finite and equal growth rates for all short waves while long waves are stable or nearly so. In this respect the exclusion of β does not change the results of the problem too much.

D) Part of the method we will use in Section 5 entails integrating across the stream. This effectively removes that region from our problem

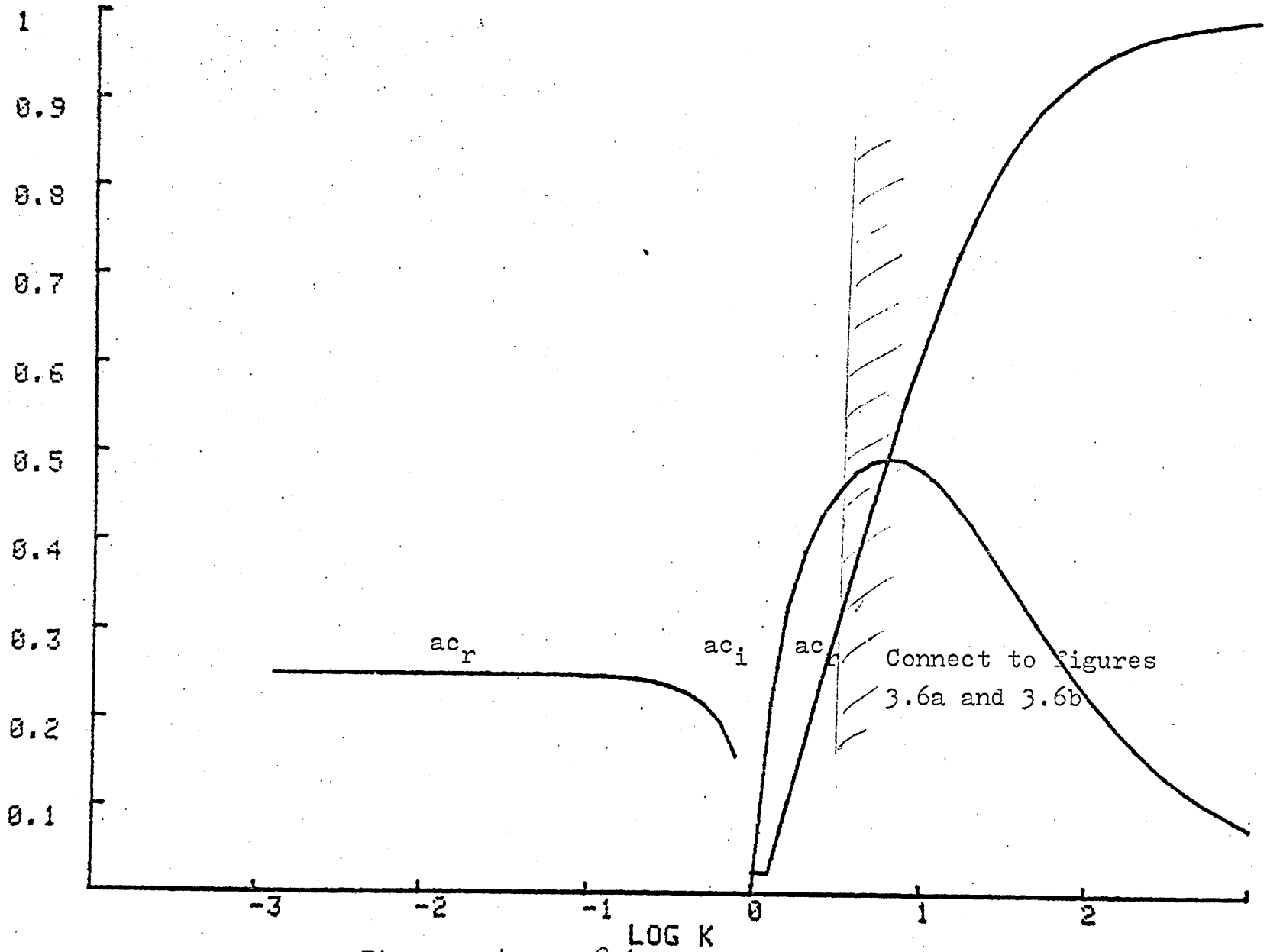

Figure 3.4 $\rho=1$

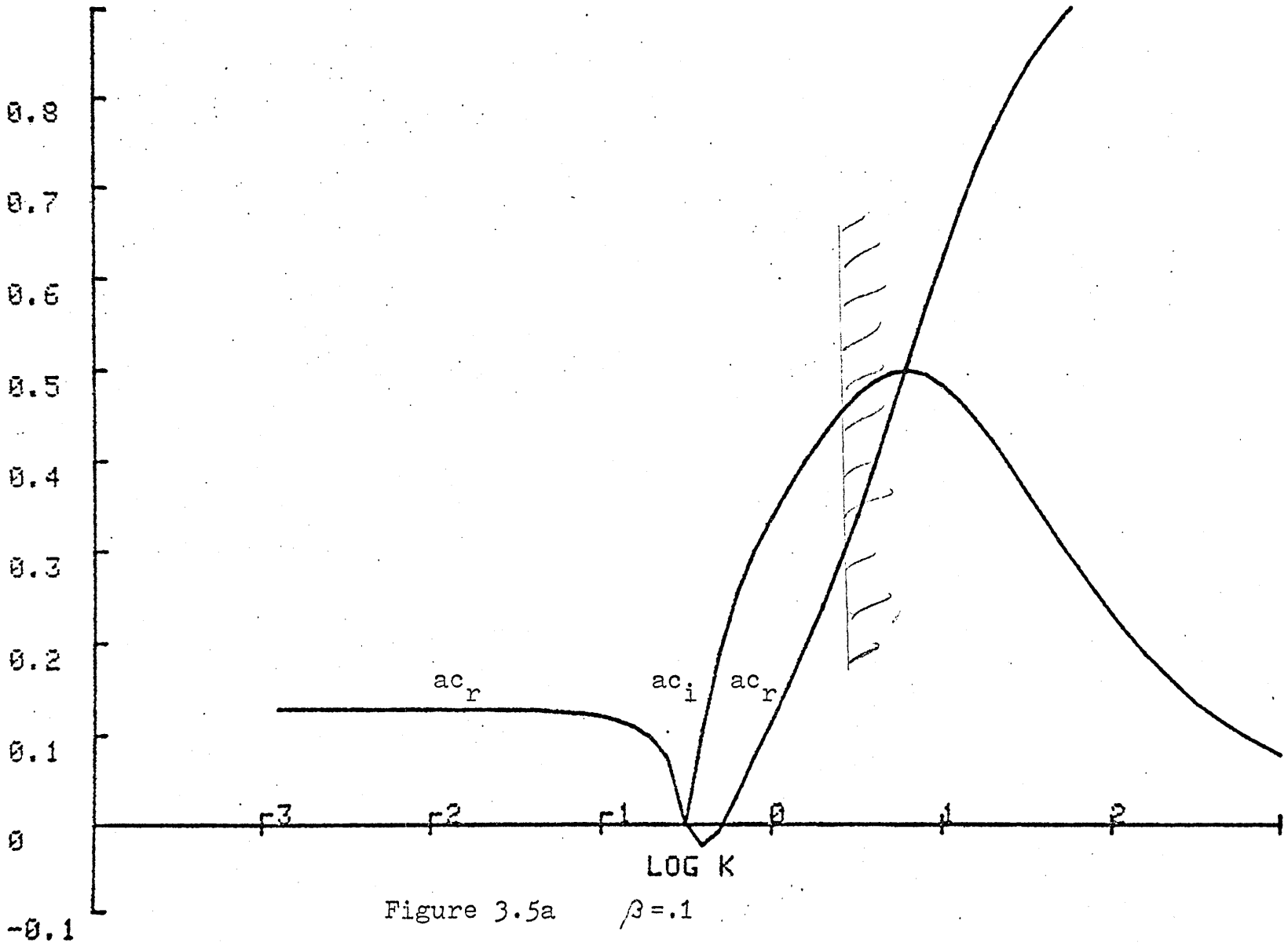

Figure 3.5a $\beta = .1$

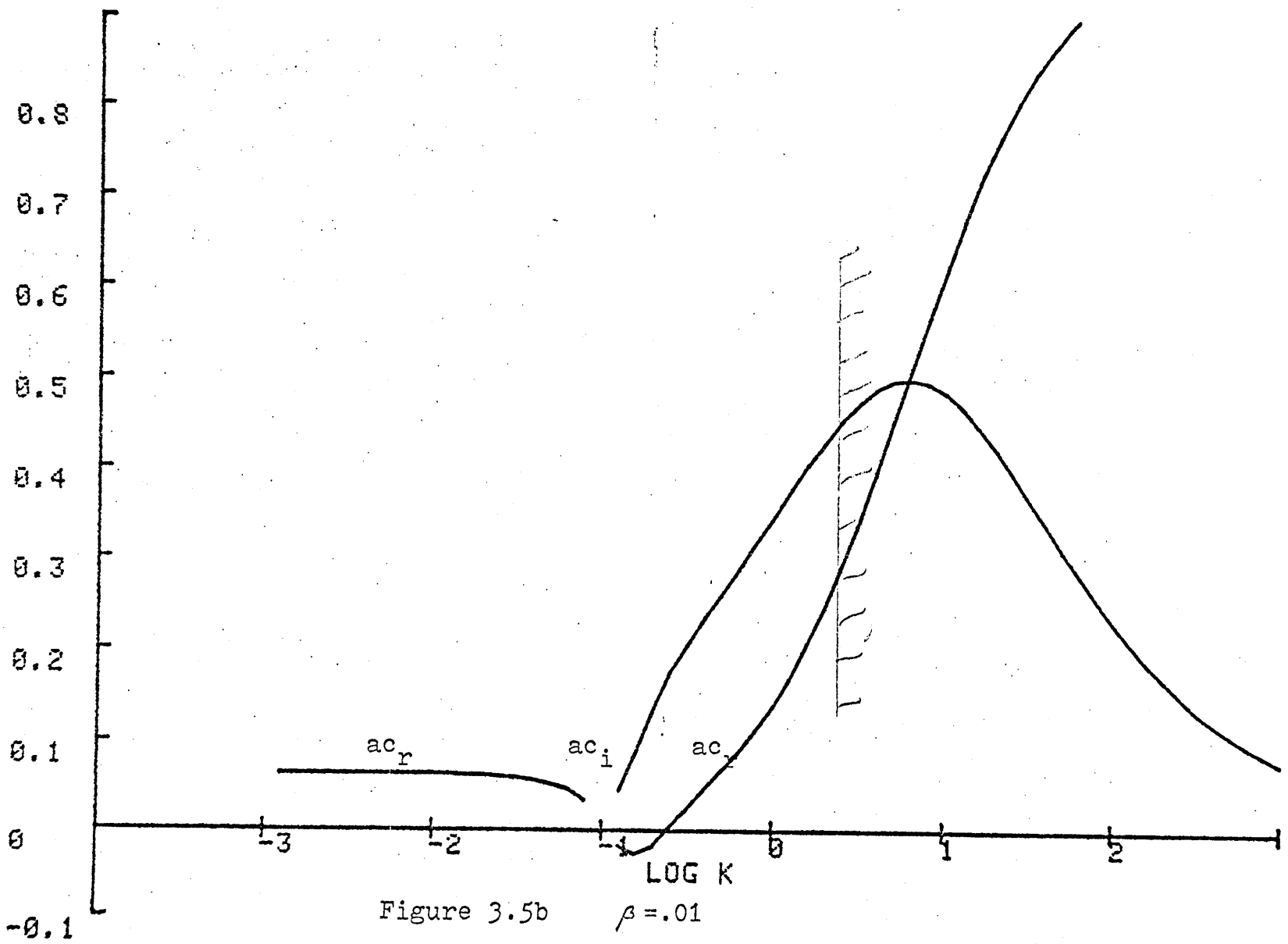

Figure 3.5b $\beta = .01$

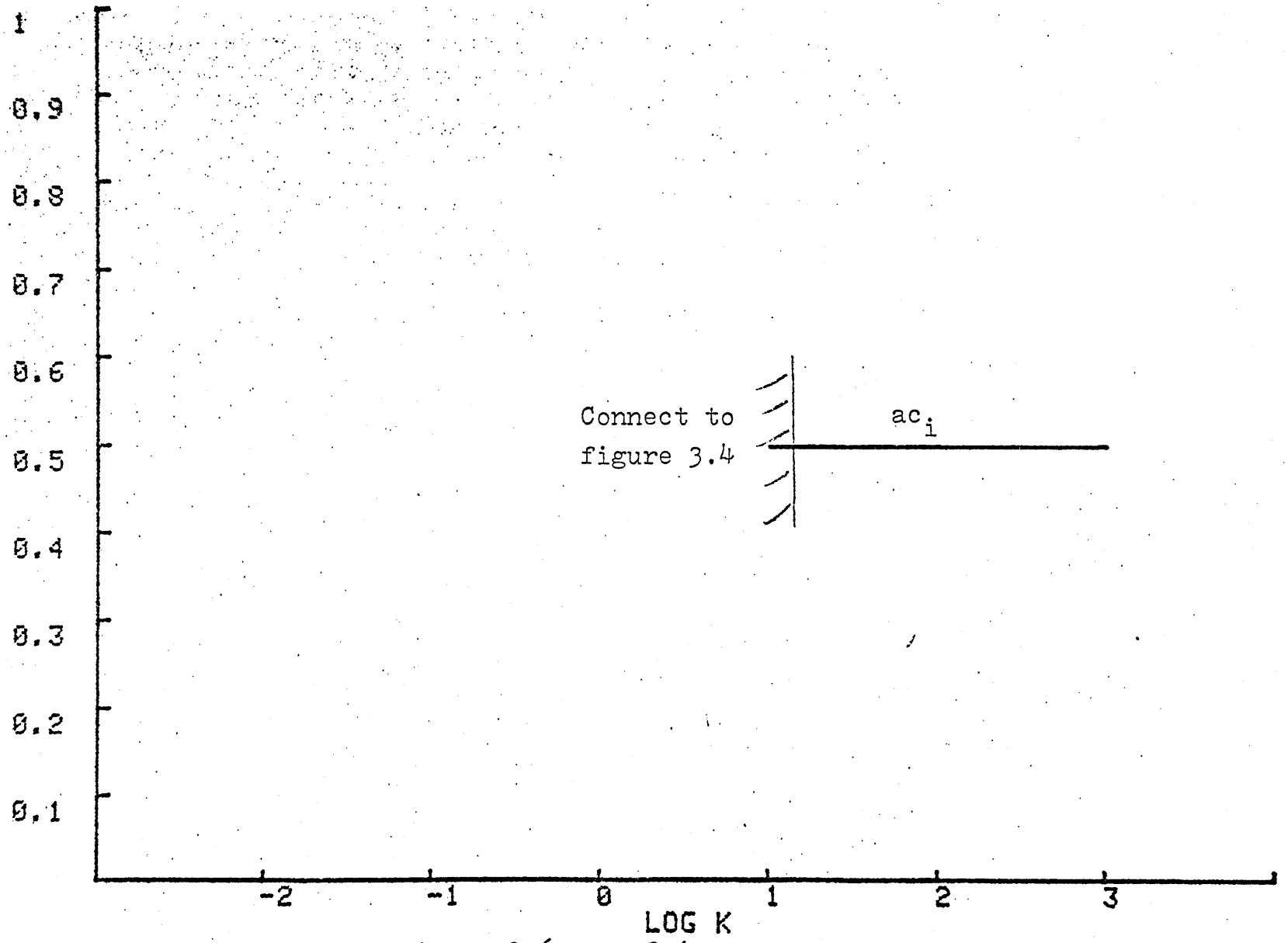

Figure 3.6a $\beta=1$

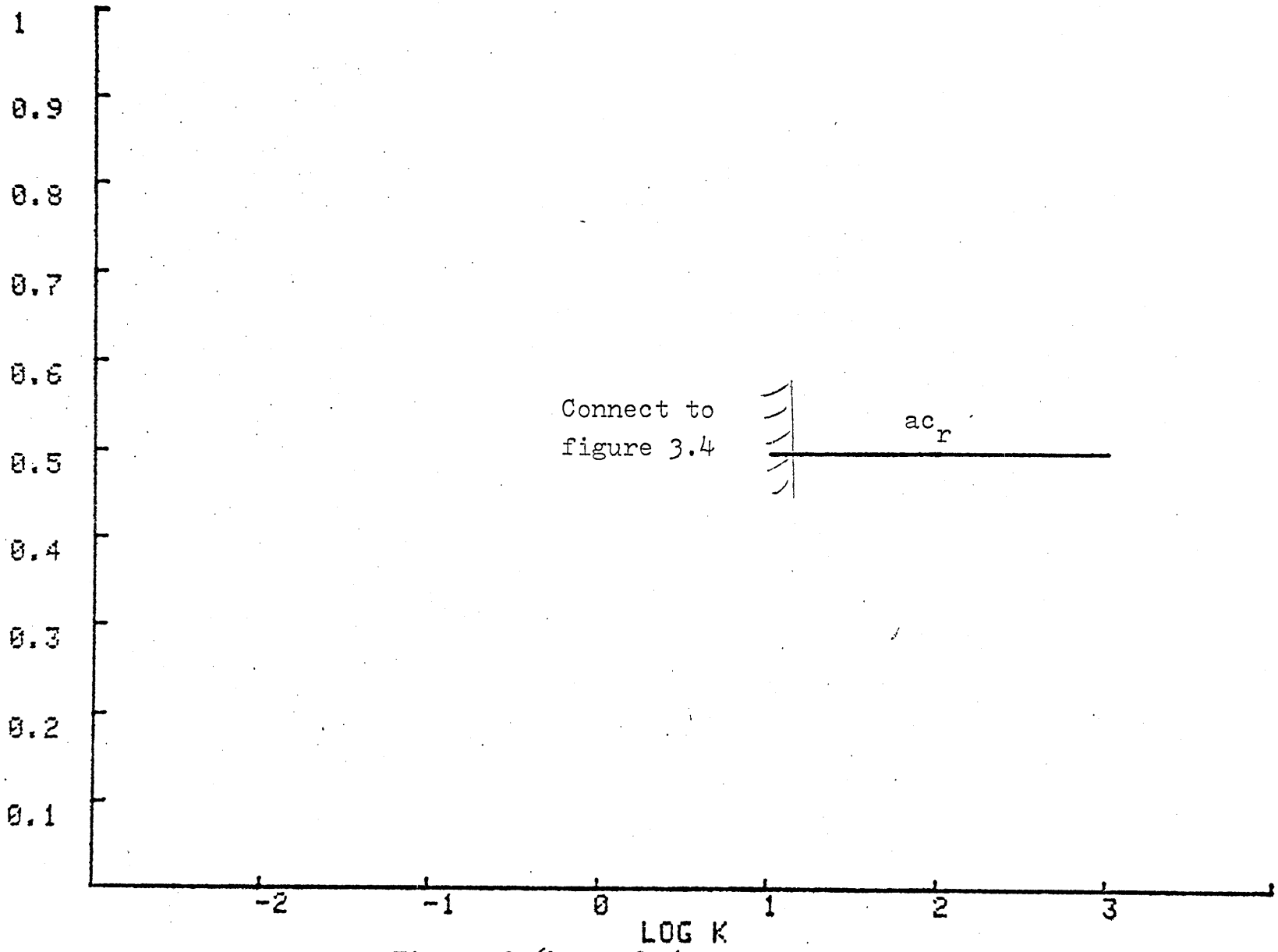

Figure 3.6b $\beta = 1$

while incorporating enough of the information from that region into a type of matching conditions on the remaining regions to solve the problem. since the jet profile there smoothly joins the quiescent ocean, there will be no actual jump conditions as there are here, but that does not affect the point we are trying to make here. Using this standard model we will see a sense in which the integrate-across-the-stream approach is similar to the standard solution. Integrating (3.6) $\int_{-1}^{1} dy$ over the jet region II gives

$$\left[(p_{II})_y\right]_{-1}^{+1} = \lambda^2\left(k^2 - \frac{\beta}{1-ac}\right)\int_{-1}^{1} p_{II}\, dy \tag{3.15}$$

If we now use the jump conditions B.9 we get

$$(p_I)_y\Big|^{+1} - (p_{III})_y\Big|^{-1} = \frac{1-ac}{ac}\lambda^2\mu_1^2\int_{-1}^{1} p_{II}\, dy \tag{3.16}$$

which, if we know p_{II}, could be viewed as an amalgamated matching condition on regions I and II. The other supermatching condition could most easily be gotten from our evenness requirement, so $p_I\big|^{+1} - p_{III}\big|^{-1} = 0$. If we now solve the governing differential equation (3.7) in the two regions, use the evenness and normalize, we get $p_I = e^{-\lambda\mu_1 y} e^{ik(x-ct)}$, $y > 1$ and $p_{III} = e^{+\lambda\mu_1 y} e^{ik(x-ct)}$, $y < 1$, where c (and hence μ_1) are still to be determined. Plugging these into (3.16) gives

$$-2\lambda\mu_1 e^{-\lambda\mu_1} = \frac{1-ac}{ac}\lambda^2\mu_1^2\int_{-1}^{1} p_{II}\, dy \tag{3.17}$$

Equation (3.17) is an equation for the eigenvalues c independent of the eigenfunctions of the remaining regions p_I and p_{III}, but it is not really an eigenequation, as p_{II} is unknown. Knowing how to get p_{II} from a full solution, as before, we can plug back into (3.17) and show we recover (3.10). The point, of course, is not that this convoluted

approach is the way to solve the linear problem, but rather that (3.17), the result of a cross stream integration, has the information in it that (3.10) has, though in a form that takes additional information to recover. Section 5 will go about justifying the cross stream integration approach in a different way: by showing that a dispersion relation analagous to (3.10) can be obtained using it and solutions to regions I and III in the linear case. This subsection is intended then only to give some insight into what is happening with the information in the equations when we use that approach.

We can now go on to build our model.

4. Formulation of the Fully Nonlinear Problem

In this section we will generate the new approach that will let us go into the nonlinear range. We will develop a governing equation and a sketch of how we will numerically work on it in a subsequent paper. As indicated in the introduction we will work with a particular set of coordinates, which we will call intrinsic coordinates. We believe that they can be applied fruitfully to other problems, such as nonlinear internal waves. They were first introduced by RN (1967), and in their full time-dependent form by RLF (1975). In Section 4A below, in the belief that they are very foreign to most readers, we develop these coordinates and the fluid dynamic equations in them in more detail than has been done in the literature. Our scaling is similar to that in RLF, but different in one very important way, one that we will see changes the entire problem. Their scaling allowed them to decouple the dynamics of the jet from the far field motion to leading order, greatly simplifying the problem. We will see for consistency that we need to retain the far field motion in the problem. In Section 4B we present a simplified form of a proof by Flierl and Robinson (to be published) showing that the scaling in RLF was inconsistent, and see what consistent scaling leaves us with in the jet region. We also develop results we will need in the next subsection. In Section 4C we generate a governing equation for the motion of the axis of the jet by first integrating across the stream and then using Green's formula on the far field to bring the information from there to the edge of the jet where we can use it. We stress the advantage of this Green's formula approach. The two-dimensional differential equation governing the far field would require a two-dimensional grid to solve numerically. This method reduces the numerics to evaluating

a one-dimensional line integral. Savings in computer time or equivalently greater resolution result. This same approach was used by Longuet-Higgens and Cokelet(1976;LC) on surface gravity waves. Another use for this would be for nonlinear internal waves, though the extension from surface waves is not trivial. Besides providing the basis for the present work, we hope the brief outline will stimulate the use of this method in other appropriate oceanographic problems.

A) The equations defining the transformation from Cartesian coordinates (x,y,t) to intrinsic coordinates (Ξ, η, t) (see Figure 4.1) are

$$x = \Xi(x,y,t) + \eta(x,y,t)\sin\theta(x,y,t) \tag{4.1}$$

$$y = \Upsilon(\Xi(x,y,t),t) - \eta(x,y,t)\cos\theta(x,y,t) \tag{4.2}$$

$$t = t \tag{4.3}$$

Instead of introducing a new time coordinate in the new system we have used the same symbol t. This conforms to RLF, but we must keep in mind that $\partial/\partial t$ is not the same in the two systems, as we will see below.

The line $y = \Upsilon(\Xi,t)$ is the moving $\eta = 0$ axis for the Ξ,η system. Below we will also identify it with the axis of the jet in the problem. We will refer to it as the axis. The normal from (x,y) to the axis intersects it at $\Xi(x,y,t)$ and has a length $|\eta(x,y,t)|$. $\theta(x,y,t)$ gives the angle between the tangent to the path at $\Xi(x,y,t)$ and east, that is,

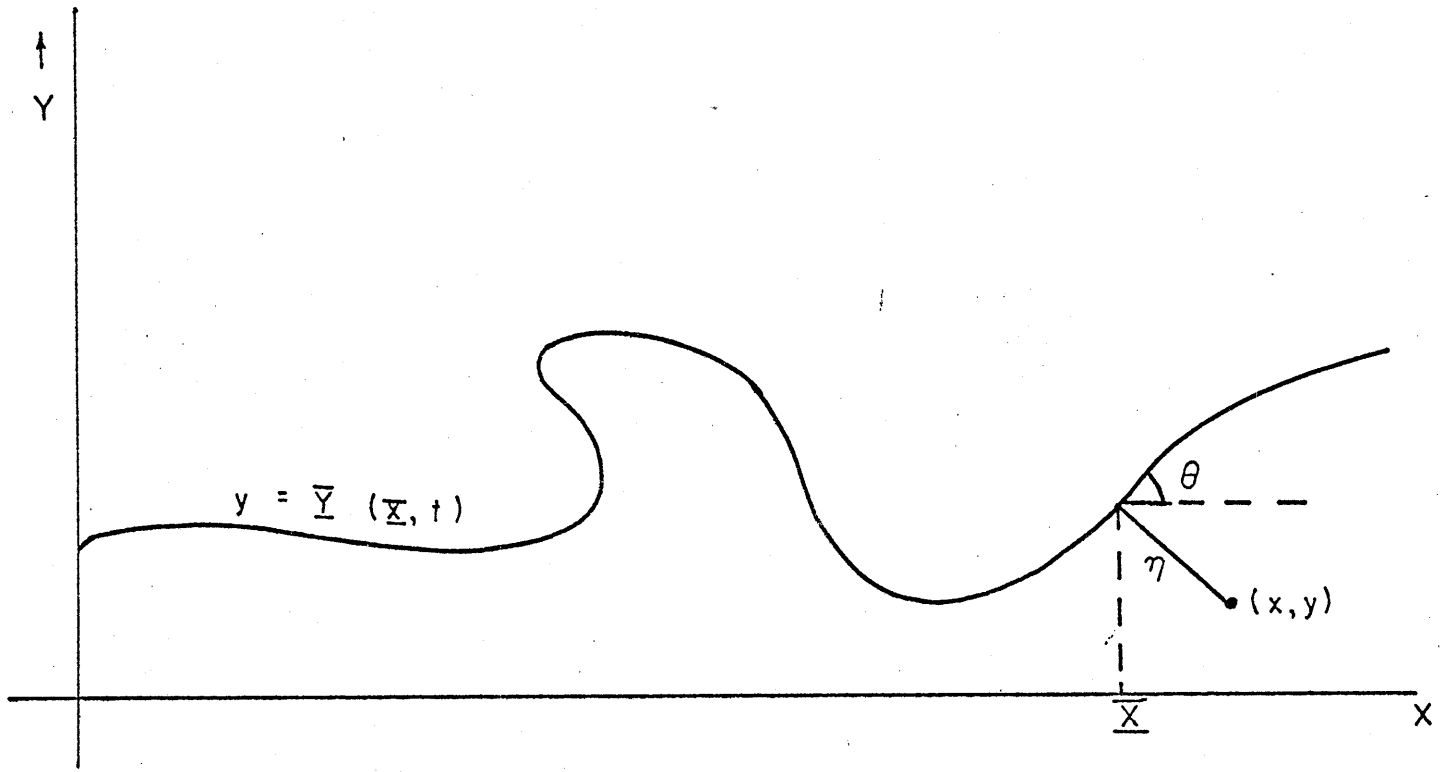

Figure 4.1

$$\Theta(x,y,t) = tan^{-1}\left(\frac{\partial Y}{\partial X}\right) \tag{4.4}$$

To investigate the 1-to-1 nature of the transformation we look at the Jacobian

$$J = \left| \frac{\partial(x,y)}{\partial(\eta,X)} \right| = \left| \frac{\partial x}{\partial \eta}\frac{\partial y}{\partial X} - \frac{\partial x}{\partial X}\frac{\partial y}{\partial \eta} \right| \tag{4.5}$$

To compute these terms we must express (4.1) and (4.2) in terms of the two variables X and η

$$x = X + \eta \frac{\partial Y/\partial X}{\sqrt{1+(\partial Y/\partial X)^2}} \tag{4.6}$$

$$y = Y(X,t) - \eta \frac{1}{\sqrt{1+(\partial Y/\partial X)^2}} \tag{4.7}$$

Noting that the curvature is $\kappa(X,t) = \frac{\partial^2 Y}{\partial X^2}\left(1+\left(\frac{\partial Y}{\partial X}\right)^2\right)^{-3/2}$ we get

$$J = \frac{1}{\cos\Theta}(1+\eta\kappa) \tag{4.8}$$

which says that for $|\eta| < |\kappa|^{-1}$ the transformation is 1 to 1. We will label

$$h \triangleq 1+\eta\kappa \tag{4.9}$$

which will be a measure of the crowding of coordinate lines. Relations between Y, Θ, and κ that will be used in the algebra below and are here listed for reference are $\dot{\Theta} = \dot{Y}'/[1+(Y')^2] = \dot{Y}'\cos^2\Theta$, $\Theta'\cos\Theta = \kappa = \dot{Y}''\cos^3\Theta$

Below we will work with flows which have w = 0 and are independent of z, but we will carry these terms for a while to keep the transformations general for later extensions to baroclinic fields. So along with (4.1) and (4.2) (we still have $X = X(x,y,t)$, etc) and (4.3) we have

$$z = z \tag{4.10}$$

again using one symbol for both systems, though here it is also true that $\partial/\partial z$ is the same in both, as z is independent of the other coordinates.

The usual Cartesian velocities $\vec{u} = (u, v, w)$ will transform to components perpendicular to and tangent to the interface

$$w = w \tag{4.11}$$

$$v = u \sin\Theta - v \cos\Theta \tag{4.12}$$

$$u = u \cos\Theta + v \sin\Theta \tag{4.13}$$

For use later, the inverse transformations are

$$u = u \cos\Theta + v \sin\Theta \tag{4.14}$$

$$v = u \sin\Theta - v \cos\Theta \tag{4.15}$$

From the definition of Θ, (4.4), we see that like Ψ it can be thought of as a function of either set of coordinates, giving $\Theta(x, y, t)$ or $\Theta(\Xi, \eta, t)$. But from the definition, because Ξ is independent of η, Θ must be also, so in intrinsic coordinates $\Theta = \Theta(\Xi, t)$.

We now move on to dynamics. In Cartesian coordinates the Boussinesq, hydrostatic, inviscid equations on the f plane ($f = f_o$) or β plane ($f = f_o + \beta y$) for the conservation of mass, momentum, and density (entropy)

$$\frac{\partial u}{\partial x} + \frac{\partial v}{\partial y} + \frac{\partial w}{\partial z} = 0 \tag{4.16}$$

$$\frac{Du}{Dt} - fv + \frac{1}{\rho_0}\frac{\partial p}{\partial x} = 0 \tag{4.17}$$

$$\frac{Dv}{Dt} + fu + \frac{1}{\rho_0}\frac{\partial p}{\partial y} = 0 \tag{4.18}$$

$$\frac{\partial p}{\partial z} - \rho_0 g s = 0 \tag{4.19}$$

$$\frac{Ds}{Dt} = 0 \tag{4.20}$$

where s is the nondimensional density anomaly, $\rho = \rho_0(1-s)$ and D/Dt is the advective derivative

$$\frac{D}{Dt} = \frac{\partial}{\partial t} + u\frac{\partial}{\partial x} + v\frac{\partial}{\partial y} + w\frac{\partial}{\partial z} \tag{4.21}$$

We will now carefully transform the two momentum equations into intrinsic coordinates. The other transformations will be similar but simpler and only the results will be given. The z coordinate will often not be written when it plays no role in what we are looking at. The case for a fixed curved wall was first done by Goldstein (1938, p.119), though he does not discuss what to do where it ceases being 1 to 1. One could simply apply the standard coordinate transformation rules (Hildebrand, Chapter 7) such as $\frac{\partial}{\partial x} = \left(1/\frac{\partial(x,y)}{\partial(\eta,\Xi)}\right)\frac{\partial y}{\partial \Xi}\frac{\partial}{\partial \eta} - \left(1/\frac{\partial(x,y)}{\partial(\eta,\Xi)}\right)\frac{\partial y}{\partial \eta}\frac{\partial}{\partial \Xi}$, but we will do things out in a more pedantic way that also makes clearer

the change in the time derivative and what it means. The first step will be re-expressing D/Dt. Observe that

$$\left.\frac{\partial}{\partial x}\right|_{y,t} F(\Xi,\eta,t) = \left.\frac{\partial F}{\partial \Xi}\right|_{\eta,t} \left.\frac{\partial \Xi}{\partial x}\right|_{y,t} + \left.\frac{\partial F}{\partial \eta}\right|_{\Xi,t} \left.\frac{\partial \eta}{\partial x}\right|_{y,t} \tag{4.22}$$

$$\left.\frac{\partial}{\partial y}\right|_{x,t} F(\Xi,\eta,t) = \left.\frac{\partial F}{\partial \Xi}\right|_{\eta,t} \left.\frac{\partial \Xi}{\partial y}\right|_{x,t} + \left.\frac{\partial F}{\partial \eta}\right|_{\Xi,t} \left.\frac{\partial \eta}{\partial y}\right|_{x,t} \tag{4.23}$$

If we now differentiate (4.1) and (4.2) with respect to x, for fixed y and t, we get, recalling $\Theta = \Theta(\Xi,t)$,

$$1 = \frac{\partial \Xi}{\partial x} + \frac{\partial \eta}{\partial x} \sin\Theta + \eta \cos\Theta \frac{\partial \Theta}{\partial \Xi} \frac{\partial \Xi}{\partial x} \tag{4.24}$$

$$0 = \frac{\partial Y}{\partial \Xi} \frac{\partial \Xi}{\partial x} - \frac{\partial \eta}{\partial x} \cos\Theta + \eta \sin\Theta \frac{\partial \Theta}{\partial \Xi} \frac{\partial \Xi}{\partial x} \tag{4.25}$$

These can be solved for $\partial\Xi/\partial x$ and $\partial\eta/\partial x$ to give

$$\left.\frac{\partial \Xi}{\partial x}\right|_{y,t} = \frac{\cos^2\Theta}{1+\eta\kappa} = \frac{\cos^2\Theta}{h} \tag{4.26}$$

$$\left.\frac{\partial \eta}{\partial x}\right|_{y,t} = \sin\Theta \tag{4.27}$$

Likewise, we differentiate (4.1) and (4.2) with respect to y and solve the matrix as above to get

$$\left.\frac{\partial \Xi}{\partial y}\right|_{x,t} = \sin\Theta \frac{\cos\Theta}{h} \tag{4.28}$$

$$\left.\frac{\partial \eta}{\partial y}\right|_{x,t} = -\cos\Theta \tag{4.29}$$

Dropping the dummy function F, we can write (4.22) and (4.23), using (4.26) and (4.27), as the operators:

$$\frac{\partial}{\partial x}\Big|_{y,t} = \cos\Theta \frac{\cos\Theta}{h} \frac{\partial}{\partial \Xi}\Big|_{\eta,t} + \sin\Theta \frac{\partial}{\partial \eta}\Big|_{\Xi,t} \tag{4.30}$$

$$\frac{\partial}{\partial y}\Big|_{x,t} = \sin\Theta \frac{\cos\Theta}{h} \frac{\partial}{\partial \Xi}\Big|_{\eta,t} + \cos\Theta \frac{\partial}{\partial \eta}\Big|_{\Xi,t} \tag{4.31}$$

Now one can recognize the spatial transformation as a rotation (where $\frac{\cos\Theta}{h}\frac{\partial}{\partial \Xi}$ gives the tangential derivative).

We can deal similarly with the less common change of $\partial/\partial t\,|_{x,y}$

$$\frac{\partial}{\partial t}\Big|_{x,y} F(\Xi,\eta,t) = \frac{\partial F}{\partial t}\Big|_{\Xi,\eta} + \frac{\partial F}{\partial \Xi}\Big|_{\eta,t}\frac{\partial \Xi}{\partial t}\Big|_{x,y} + \frac{\partial F}{\partial \eta}\Big|_{\Xi,t}\frac{\partial \eta}{\partial t}\Big|_{x,y} \tag{4.32}$$

We can hit (4.1) and (4.2) by $\partial/\partial t\,|_{x,y}$ and for now represent $\partial/\partial t|_{x,y}$ by ".".

$$0 = \dot{\Xi} + \dot{\eta}\sin\Theta + \eta\cos\Theta\left(\frac{\partial\Theta}{\partial\Xi}\dot{\Xi} + \frac{\partial\Theta}{\partial t}\Big|_{\Xi}\right) \tag{4.33}$$

$$0 = \frac{\partial Y}{\partial t}\Big|_{\Xi} + \frac{\partial Y}{\partial \Xi}\dot{\Xi} - \dot{\eta}\sin\Theta\left(\frac{\partial\Theta}{\partial\Xi}\dot{\Xi} + \frac{\partial\Theta}{\partial t}\Big|_{\Xi}\right) \tag{4.34}$$

Solving these for $\dot{\Xi}$ and $\dot{\eta}$ gives

$$\dot{\Xi} = \frac{\cos\Theta}{h}\left(\sin\Theta\frac{\partial Y}{\partial t}\Big|_{\Xi} - \eta\frac{\partial\Theta}{\partial t}\Big|_{\Xi}\right) \tag{4.35}$$

$$\dot{\eta} = \cos\Theta\frac{\partial Y}{\partial t}\Big|_{\Xi} \tag{4.36}$$

Plugging (4.35) and (4.36) into (4.32) and then changing symbols so "." = $\partial/\partial t\,|_{\Xi}$ we get

$$\left.\frac{\partial}{\partial t}\right|_{x,y} = \left.\frac{\partial}{\partial t}\right|_{\xi,\eta} + \left(\dot{Y}\sin\theta - \eta\dot{\theta}\right)\frac{\cos\theta}{h}\left.\frac{\partial}{\partial \xi}\right|_{\eta,t} + \left(\dot{Y}\cos\theta\right)\left.\frac{\partial}{\partial \eta}\right|_{\xi,t} \tag{4.37}$$

From (4.37) we will be able to tell at a glance, below when we write the advective derivative in these coordinates, which parts come from the old but in the new system look like advective terms.

Bringing together (4.21), (4.37), (4.14), (4.15), (4.30) and (4.31) gives

$$\frac{D}{Dt} = \frac{\partial}{\partial t} + (v + \dot{Y}\cos\theta)\frac{\partial}{\partial \eta} + \left(u - \dot{Y}\sin\theta - \eta\dot{\theta}\right)\frac{\cos\theta}{h}\frac{\partial}{\partial \xi} + w\frac{\partial}{\partial z} \tag{4.38}$$

Now to tackle the momentum equations. Using (4.14) and (4.15) to substitute for u and v and (4.30) for $\partial/\partial x|_{y,t}$ in (4.17), and noting that our operatore (4.38) obeys the usual rule for products and the chain rule, gives

$$\sin\theta\frac{Du}{Dt} + u\cos\theta\frac{D\theta}{Dt} - \cos\theta\frac{Dv}{Dt}$$

$$+ v\sin\theta\frac{D\theta}{Dt} - f\left(u\cos\theta + v\sin\theta\right) = -\frac{1}{\rho_0}\left(\frac{\cos^2\theta}{h}\frac{\partial}{\partial \xi} + \sin\theta\frac{\partial}{\partial \eta}\right)p \tag{4.39}$$

Similarly, (4.18) becomes

$$\cos\theta\frac{Du}{Dt} - u\sin\theta\frac{D\theta}{Dt} + \sin\theta\frac{Dv}{Dt}$$

$$+ v\cos\theta\frac{D\theta}{Dt} + f\left(u\sin\theta - v\cos\theta\right) = -\frac{1}{\rho_0}\left(\sin\theta\frac{\cos\theta}{h}\frac{\partial}{\partial \xi} - \cos\theta\frac{\partial}{\partial \eta}\right)p \tag{4.40}$$

Adding $\cos\theta$ times (4.40) to $\sin\theta$ times (4.39) gives

$$\frac{Du}{Dt} + v\frac{D\theta}{Dt} + fv = -\frac{1}{\rho_0}\frac{\cos\theta}{h}\frac{\partial p}{\partial \xi} \tag{4.41}$$

Substracting $\cos\theta$ times (4.39) from $\sin\theta$ times (4.40) gives

$$\frac{Dv}{Dt} - u\frac{D\theta}{Dt} - fu = -\frac{1}{\rho_0}\frac{\partial p}{\partial \eta} \tag{4.42}$$

We have then a remarkably small change in the form of the momentum equations.

Equations (4.16), (4.19) and (4.20) become, respectively,

$$\frac{\partial v}{\partial \eta} + \frac{\chi}{h}v + \frac{\cos\theta}{h}\frac{\partial u}{\partial \xi} + \frac{\partial w}{\partial z} = 0 = \frac{1}{h}\frac{\partial}{\partial \eta}(hv) + \frac{\cos\theta}{h}\frac{\partial u}{\partial \xi} + \frac{\partial w}{\partial z} \tag{4.43}$$

$$\frac{\partial p}{\partial z} = \rho_0 g \tag{4.44}$$

$$\frac{Ds}{Dt} = 0 \tag{4.45}$$

Next, from the basic equations, we will form the equation which will be key for us, the vorticity equation (of course, we could have transformed the Cartesian vorticity equation, but this way one gets more of a feel for the new coordinate system). From $\frac{\partial}{\partial \eta}((h)(4.41))$ we subtract $\cos\Theta\left(\frac{\partial}{\partial \Xi}(4.42)\right)$

$$\frac{\partial}{\partial \eta} h \frac{D\mu}{Dt} - \cos\Theta \frac{\partial}{\partial \Xi}\frac{D\mu}{Dt} + \frac{\partial}{\partial \eta} h\nu \frac{D\Theta}{Dt} + \cos\Theta \frac{\partial}{\partial \Xi}\mu\frac{D\alpha}{Dt} + f\left(\frac{\partial}{\partial \eta}(h\nu) + \cos\Theta \frac{\partial \mu}{\partial \Xi}\right) + h\nu \frac{\partial}{\partial \eta} f + \mu \cos\Theta \frac{\partial}{\partial \Xi} f = 0 \tag{4.46}$$

This can be rewritten in a somewhat more illuminating form as follows. We can invert (4.30) and (4.31) easily by multiplying by $\sin\Theta$ and $\cos\Theta$ and then adding and subtracting, to express $\frac{\partial}{\partial \eta}$ and $\frac{\partial}{\partial \Xi}$ in terms of $\frac{\partial}{\partial x}$ and $\frac{\partial}{\partial y}$ and then operate on $f = f_0 + \beta y$. We take an equivalent approach by leaving it with the operators it has and writing $f = 1 + \beta(\Upsilon - \eta\cos\Theta)$ using (4.2). Recalling $\Upsilon_\Xi = \tan\Theta$ and $1 + \eta\chi = h$, and applying the continuity equation (4.43) twice to the rest of the equation, our vorticity equation becomes

$$\frac{\partial}{\partial \eta} h \frac{D\mu}{Dt} - \cos\Theta \frac{\partial}{\partial \Xi}\frac{D\nu}{Dt} + \mu\cos\Theta \frac{\partial}{\partial \Xi}\frac{D\Theta}{Dt} + h\nu \frac{\partial}{\partial \eta}\frac{D\Theta}{Dt} + h\beta(\mu\sin\Theta - \nu\cos\Theta) - \left(f + \frac{D\Theta}{Dt}\right) h \frac{\partial w}{\partial z} = 0 \tag{4.47}$$

The vorticity equation in these coordinates strongly resembles in form our usual Cartesian equation. The βv effect is just the same as usual as it should be since it represents the interaction of north flow with the earth's spin and so will not be affected by local twisting. As mentioned when defined in (4.9), the h just gives a geometric effect of coordinate line crowding. In places like $\frac{\partial}{\partial \eta} h \frac{D\mu}{Dt}$ it can give rise to a term depending strongly on curvature, here $\chi \frac{D\mu}{Dt}$. This indicates that if we generate a flow along the local tangent $\hat{t}$ while $\hat{t}$ has a different

direction in space as we move along the flow, we are generating a swirling flow vorticity. The terms that look newest are those with $D\Theta/Dt$. They represent coordinate rotation and play a role much like the local vertical rotation f. We pick up exactly the Coriolis terms we would expect, as seen clearly in the momentum equations (4.41) and (4.42). In the vorticity equation their gradient enters, as with f. Also this coordinate rotation shows up in the coefficient of the stretching term, just as the rotation should.

For the rest of this work we will consider the fluid homogeneous. ρ_0 will be absorbed into the pressure p. We will take further a flat top and bottom in line with our goals outlined in the introduction so $w \equiv 0$ and z effectively drops from the problem. In the primitive equations (4.44) and (4.45) can be dropped, $\partial w/\partial z$ drops from (4.43), and $w\,\partial/\partial z$ drops from D/Dt. For our vorticity equation (4.47), the vortex stretching term drops. We have

$$\frac{\partial}{\partial \eta} h \frac{Du}{Dt} - \cos\theta \frac{\partial}{\partial x}\frac{Dv}{Dt} + u\cos\theta \frac{\partial}{\partial x}\frac{D\theta}{Dt} + hv\frac{\partial}{\partial \eta}\frac{D\theta}{Dt} + h\beta(u\sin\theta - v\cos\theta) = 0 \qquad (4.48)$$

Next, without approximations, we divide up the velocity field in the jet in a way that facilitates making approximations based on the structure of the problem, that is, that we have a strong coherent moving jet field, and based on our goal of finding the motion of the jet's axis. Let

$$u = U(\eta) + u_A(\bar{x}, t) + u_m(\bar{x}, \eta, t) \qquad (4.49)$$

$$v = v_A(\bar{x}, t) + v_m(\bar{x}, \eta, t) \qquad (4.50)$$

U is a specified background jet velocity, non-zero only between $\eta = +1$ and $\eta = -1$, which is the region we are considering here. μ_A and v_A tell how the axis moves and will be defined below. μ_m and μ_m are what is left over. We call them the "meander-induced" fields.

We will now scale our equations and go to nondimensional variables. Let

$\eta \sim \ell$, the width of our firehose jet

$X, Y \sim \mathcal{L}$, a characteristic length for downstream meanders

Notice that it follows that the curvature K has a scale $\kappa \sim 1/\mathcal{L}$

$t \sim T$, a characteristic time scale for meandering

$U(\eta) \sim V_0$, a scale for the "background" jet velocity

$v_A, \mu_A \sim V_A$, a characteristic velocity scale for the axis motion

But our time and one-length scale are defined in terms of the axis motion already, so for consistency we must have $V_A = \mathcal{L}/T$

$\mu_m \sim V_m$, a velocity scale for the tangential meander-induced field in the jet

$v_m \sim \frac{\ell}{\mathcal{L}} V_m$. This "leftover" motion in the jet region tends to be constrained by the geometry of the jet, so the perpendicular velocity is down by the apsect ratio.

$f (= f_0 + \beta y) \sim f_0$

We not introduce the following nondimensional parameters:

$\lambda = \ell/\mathcal{L}$, the horizontal aspect ratio

$\varepsilon = V/f_0 \mathcal{L}$, the downstream Rossby number

$a = V_A/V_0$, the relative velocity of the axis

$m = V_m/V_0$, the relative velocity of the residual field.

$\hat{\beta} = \frac{\beta \mathcal{L}}{f_0}$ where we notice the scale is $\mathcal{L}$ from y or Y , not from η . Using our values above, this parameter turns out to be about the size of ε ,

so we choose to rewrite this $\hat{\beta} = \varepsilon \tilde{\beta}$ where $\tilde{\beta} = \rho \ell^2 / V_0$ is O(1) (recall our discussion on this in Section 3).

We will now change notation to starred quantities being dimensional and unmarked quantities being nondimensional. For example, $U^* = V_0^* U$. We get

$$u^* = V_0^* \left(U(\eta) + a \mu_A(\underline{X}, t) + m \mu_m(\eta, \underline{X}, t) \right)$$

$$v^* = V_0^* \left(a \nu_A(\underline{X}, t) + m \lambda \nu_m(\eta, \underline{X}, t) \right)$$

$$h = 1 + \eta^* \mathcal{H}^* = 1 + \lambda \eta \mathcal{H}$$

$$f^* = f_0^* f = f_0^* \left(1 + \varepsilon \tilde{\beta} y \right)$$

(so on the f plane, f $\equiv$ 1)

We will scale the pressure geostrophically cross-stream, where the sharper gradients occur, giving

$$p^* = f_0^* \ell^* V_0^* p(\eta, \underline{X}, t)$$

The convective derivative becomes

$$\left(\frac{D}{Dt}\right)^* = \frac{V_0^*}{\ell^*} \left\{ a \frac{\partial}{\partial t} + \left(U + a\mu_A + m\mu_m - a\dot{\gamma} \sin\theta - \lambda a \eta \dot{\theta} \right) \cdot \frac{\cos\theta}{h} \frac{\partial}{\partial \underline{X}} + \left(a\nu_A + m\lambda\nu_m + a\dot{\gamma}\cos\theta \right) \frac{\partial}{\partial \eta} \right\} \equiv \frac{V_0^*}{\ell^*} \frac{D}{Dt}$$

With these, our basic equations become

$$\varepsilon \left[\frac{Dv}{Dt} - u \frac{D\theta}{Dt} \right] - f u = - \frac{\partial p}{\partial \eta} \qquad (4.51)$$

$$\varepsilon\left[\frac{D\mu}{Dt}+\nu\frac{D\theta}{Dt}\right]+f\nu=-\lambda\frac{\cos\theta}{h}\frac{\partial p}{\partial X} \tag{4.52}$$

For the continuity equation we will write out the various orders, as we will have more to say on μ_A and ν_A below.

$$\frac{\partial}{\partial\eta}\left(a\nu_A+\lambda m\nu_m\right)+\lambda\frac{\partial\kappa}{h}\left(a\nu_A+\lambda m\nu_m\right)+\lambda\frac{\cos\theta}{h}\frac{\partial}{\partial X}\left(a\mu_A+m\mu_m\right)=0 \tag{4.53}$$

The vorticity equation (4.48) becomes, with scaling,

$$\frac{\partial}{\partial\eta}h\frac{D\mu}{Dt}-\lambda\cos\theta\frac{\partial}{\partial X}\frac{D\nu}{Dt}+h\nu\frac{\partial}{\partial\eta}\frac{D\theta}{Dt}+\lambda\mu\cos\theta\frac{\partial}{\partial X}\frac{D\theta}{Dt}+\lambda h\tilde{\beta}\left(\mu\sin\theta-\nu\cos\theta\right)=0 \tag{4.54}$$

or, a form we will sometimes find more useful

$$\frac{\partial}{\partial\eta}h\frac{D\mu}{Dt}-\lambda\cos\theta\frac{\partial}{\partial X}\frac{D\nu}{Dt}+\frac{\partial}{\partial\eta}h\nu\frac{D\theta}{Dt}+\lambda\cos\theta\frac{\partial}{\partial X}\mu\frac{D\theta}{Dt}+\lambda h\tilde{\beta}\left(\mu\sin\theta-\nu\cos\theta\right)=0 \tag{4.55}$$

We will now re-express μ_A and ν_A in terms of the position of the axis and its derivatives.

We will adopt from RLF their first requirement, that a particle acted on by just the axis field will stay on the axis. We get then

$$\frac{D_A}{Dt}\left(Y-\bar{Y}(X,t)\right)=0 \tag{4.56}$$

which can be worked on in either coordinate system. The result, giving the normal motion of the axis, is

$$\nu_A=-\dot{Y}\cos\theta \tag{4.57}$$

which is also the velocity for any line of constant η, including the two which mark the edge of the jet, $\eta=\pm1$.

Some type of additional assumption will need to be made to express μ_A uniquely. We restress that we are only dividing up the motion at this

point, different choices might be more or less convenient, they will change what part of the motion is in μ_A and what is not, but they cannot affect the total μ which the solution of the problem will give.

The bunching of particles on the interface in the work by Longuet-Higgins and Cokelet (1976; LC), a paper that used the Green's formula approach on a very different problem, warns us that the assumption of inextensibility found useful by RLF may not be useful for us. We therefore simply divide the tangential motion of particles connected with axis motion into two parts, the one from the projection of the axis motion, the other anything else. Our work in this paper will not require that we be more specific. We will return to this when needed in future papers.

$$\mu_A(\bar{X},t) = \dot{\gamma}\sin\theta + \psi(\bar{X},t) \tag{4.58}$$

Requiring a geostrophic balance for all three pieces of the velocity field (so $\varepsilon \ll a, \lambda, m$) will tell us about p. From (4.51) and (4.52)

$$-\left(U + a\mu_A + m\mu_m\right) = -\frac{\partial p}{\partial \eta} \tag{4.59}$$

$$\left(a\nu_A + \lambda m \nu_m\right) = -\frac{\cos\theta}{h}\frac{\partial p}{\partial \bar{X}} \tag{4.60}$$

We can now see that an appropriate expansion for the nondimensional p would be

$$p(\eta,\bar{X},t) = p_J(\eta) + \frac{a}{\lambda}p_A(\lambda\eta,\bar{X},t) + m p_m(\eta,\bar{X},t) \tag{4.61}$$

Then

$$U(\eta) = \frac{\partial p_J}{\partial \eta} \tag{4.62}$$

$$\mu_A(\bar{X},t) = \frac{\partial P_A}{\partial \eta}(\lambda\eta, \bar{X}, t) \tag{4.63}$$

$$v_A(\bar{X},t) = -\frac{\cos\Theta}{h}\frac{\partial}{\partial \bar{X}} P_A(\lambda\eta, \bar{X}, t) \tag{4.64}$$

What this axis field balance is trying to tell us is, that since μ_A and v_A were assumed to be the same size, not being constrained by the jet geometry, when they are expressed geostrophically as pressure gradients based on scaling based on the jet's aspect ratio, compensation must be made. The dimensional quantities $\partial P_A^*/\partial \lambda^*$ and $-\frac{\cos\Theta}{h}\frac{\partial P_A^*}{\partial \eta^*}$ are both made to scale to a by scaling $\partial P_A^*/\partial \eta^*$ as $f_o^* \ell^* V_o^* a/\ell^*\lambda$ instead of just $f_o^* \ell^* V_o^* a/\ell^*$. In nondimensional form to fix up $\partial P/\partial \eta$ means P_A depends on $\lambda\eta$ as indicated. Note that this is all consistent with the results that RLF get, though they express their vorticity equation in terms of Y and its derivatives (if one tries to compare, be careful, they lose some λ's in some equations which reappear later correctly). Below we use the expression of P_A they wrote explicitly, and we will see that it has just the form discussed.

At order m,

$$\mu_m(\eta, \bar{X}, t) = \frac{\partial P_m}{\partial \eta}(\eta, \bar{X}, t) \tag{4.65}$$

$$v_m(\eta, \bar{X}, t) = -\frac{\cos\Theta}{h}\frac{\partial P_m}{\partial \bar{X}}(\eta, \bar{X}, t) \tag{4.66}$$

B) $\beta=0$ for the rest of this paper. We present a simplified form of the demonstration in FR that the ordering of parameters assumed in RLF

is inconsistent, and what balance a consistent scaling leads to. Mathematically, the upshot is that the motion of the axis can no longer be determined to leading order just from the dynamics of the stream, but one must consider the motion of the far fields too, leading to a much more complicated problem. We will also use some of the results here in the following sections.

We will first divide the nondimensional D/Dt into what might be thought of as lower order and higher order operators

$$\frac{D}{Dt} = \left\{ a\frac{\partial}{\partial t} + \left(U + a(\dot{\gamma}\sin\theta + \psi) + m\mu_m - a\dot{\gamma}\sin\theta - \lambda a\eta\dot{\theta}\right)\cdot \right. \tag{4.67}$$

$$\left. \cdot \frac{\cos\theta}{1+\lambda\eta\kappa}\frac{\partial}{\partial X} + \left(a(-\dot{\gamma}\cos\theta) + m\nu_m + a\dot{\gamma}\cos\theta\right)\frac{\partial}{\partial\eta}\right\}$$

$$= \left\{ a\frac{\partial}{\partial t} + (U+a\psi)\cos\theta\frac{\partial}{\partial X}\right\} + m\left\{ \left(\mu_m - \frac{\lambda}{m}a\eta\dot{\theta} - \frac{\lambda}{m}\eta\kappa(U+a\psi)\cdot\right.\right.$$

$$\left.\left. \cdot\cos\theta\frac{\partial}{\partial X} + \nu_m\frac{\partial}{\partial\eta}\right\} \triangleq \frac{D_0}{Dt} + m\frac{D_1}{Dt}$$

A result we will use in the expansion below is

$$a\frac{\partial}{\partial\eta}h\frac{D_0}{Dt}\mu_A + ah\nu_A\frac{\partial}{\partial\eta}\frac{D_0}{Dt}\theta = a\lambda\kappa\frac{D_0}{Dt}\mu_A \tag{4.68}$$

$$+ah\frac{\partial}{\partial\eta}\left(a\frac{\partial}{\partial t} + (U+a\psi)\cos\theta\frac{\partial}{\partial X}\right)\mu_A + ah\nu_A\frac{\partial}{\partial\eta}\left(a\frac{\partial}{\partial t} + (U+a\psi)\cos\theta\frac{\partial}{\partial X}\right)$$

$$= a\lambda\kappa\left(a\mu_{At} + (U+a\psi)\cos\theta\mu_{AX}\right) + ah\upsilon_\eta\cos\theta\mu_{AX} + ah\nu_A\upsilon_\eta\cos\theta\theta_X$$

$$= a\lambda\kappa\left(a\mu_{At} + (U+a\psi)\cos\theta\mu_{AX}\right)$$

where we used $\cos\theta\,\theta_X = \kappa$ and the continuity equation in the last step.

Now, recalling $U = U(\eta)$ and so is unaffected by D_0/Dt, we will expand the vorticity equation (4.54)

$$0 = \frac{\partial}{\partial\eta}h\frac{D_0}{Dt}\mu_A + m\frac{\partial}{\partial\eta}h\frac{D_0}{Dt}\mu_m + m\frac{\partial}{\partial\eta}h\frac{D_1}{Dt}(U+a\mu_A) + m^2\frac{\partial}{\partial\eta}h\frac{D_1}{Dt}\mu_m \tag{4.69}$$

$$-\lambda a\cos\theta\frac{\partial}{\partial X}\frac{D_0}{Dt}\nu_A - \lambda^2 m\cos\theta\frac{\partial}{\partial X}\frac{D_0}{Dt}\nu_m - a\lambda m\cos\theta\frac{\partial}{\partial X}\frac{D_1}{Dt}\nu_A - \lambda^2 m^2\cos\theta\frac{\partial}{\partial X}\frac{D_1}{Dt}\nu_m$$

$$+\lambda(U+\gamma\mu_A)\cos\theta\frac{\partial}{\partial\Sigma}\frac{D_0}{Dt}\Theta+\lambda m\mu_m\cos\theta\frac{\partial}{\partial\Sigma}\frac{D_0}{Dt}\Theta+m\lambda(U+\gamma\mu_A)\cos\theta\frac{\partial}{\partial\Sigma}\frac{D_1}{Dt}\Theta+m^2\lambda\mu_m\cos\theta\frac{\partial D_0\Theta}{\partial\Sigma Dt}$$

$$h\alpha\nu_A\frac{\partial}{\partial\eta}\frac{D_0}{Dt}\Theta+\lambda mh\nu_m\frac{\partial}{\partial\eta}\frac{D_0}{Dt}\Theta+\alpha mh\nu_A\frac{\partial}{\partial\eta}\frac{D_1}{Dt}\Theta+\lambda m^2h\nu_m\frac{\partial}{\partial\eta}\frac{D_1}{Dt}\Theta$$

We will now look at $m<<1$, the assumption that the "leftover" fields in the jet are weak, and $\lambda<<1$, the assumption that the jet is thin, and look into how λ and m can be related.

The first, fifth, ninth, and thirteenth terms in (4.69) represent the axis vorticity terms. Using (4.68) we see that we can write this sum as λ times an O(1) term which following FR we call $\dot{AV}$. The second, third, sixth, seventh, tenth, eleventh, fourteenth and fifteenth terms represent the interaction of the axis and the meander fields, and we will label their sum mVI_1. The remaining four terms are the self-interaction of the meander field, and we will call their sum m^2VI_2. (4.69) can now be written

$$\dot{AV}+\frac{m}{\lambda}VI_1+\frac{m^2}{\lambda}VI_2=0 \qquad (4.70)$$

In RLF they took $m(\sim\varepsilon)<<\lambda<<1$. Then (4.70) says $\dot{AV}=0$, or, using (4.68),

$$F_0(\bar{X},t)+U(\eta)F_1(\bar{X},t)+U^2(\eta)F_2(\bar{X},t)=0 \qquad (4.71)$$

where $F_0(\bar{X},t)=\alpha^2\{\chi\left(\frac{\partial}{\partial t}+\Psi\cos\theta\frac{\partial}{\partial\bar{X}}\right)\mu_A-\cos\theta\frac{\partial}{\partial\Sigma}\cdot$

$$\cdot\left(\frac{\partial}{\partial t}+\Psi\cos\theta\frac{\partial}{\partial\bar{X}}\right)\nu_A+\mu_A\cos\theta\frac{\partial}{\partial\Sigma}\left(\frac{\partial}{\partial t}+\Psi\cos\theta\frac{\partial}{\partial\bar{X}}\right)\theta\}$$

$$F_1(\bar{X},t)=\alpha\{\chi\cos\theta\mu_{A\bar{X}}-\cos\theta\frac{\partial}{\partial\Sigma}(\cos\theta\nu_{A\bar{X}})$$

$$+\cos\theta\frac{\partial}{\partial\Sigma}\left(\frac{\partial}{\partial t}+\Psi\cos\theta\frac{\partial}{\partial\bar{X}}\right)\theta+\mu_A\cos\theta\frac{\partial}{\partial\Sigma}(\cos\theta\theta_{\bar{X}})$$

$$F_2(\bar{X},t)=\cos\theta\frac{\partial}{\partial\Sigma}(\cos\theta\theta_{\bar{X}})$$

Clearly, this balance cannot hold for arbitrary $v(\eta)$ for all η, since the terms depend differently on η. So this balance is inconsistent.

Equation (4.70) suggests the balance $m \sim \lambda << 1$. With this we get

$$\dot{A}V + VI_1 = 0 \tag{4.72}$$

and the problem of a balance for all η vanishes, for VI_1 has all the freedom needed from the μ_m and ν_m in it.

With our parameters $m \sim \lambda << 1$ we get approximately

$$\dot{A}V = a\,\mathcal{K}\left(a\mu_{A_t} + (U + a\Psi)\cos\theta\,\mu_{A_X}\right) - a\cos\theta\frac{\partial}{\partial X}\left(a\frac{\partial}{\partial t} + \right. \tag{4.73}$$

$$\left.(U+a\Psi)\cos\theta\frac{\partial}{\partial X}\right)\nu_A + (U+a\mu_A)\cos\theta\frac{\partial}{\partial X}\left(a\frac{\partial}{\partial t} + (U+a\Psi)\cos\theta\frac{\partial}{\partial X}\right)\theta$$

$$VI_1 = \frac{\partial}{\partial\eta}\left\{\left(a\frac{\partial}{\partial t} + (U+a\Psi)\cos\theta\frac{\partial}{\partial X}\right)\mu_m + \frac{D_1}{Dt}(U+a\mu_A) + a\nu_A\frac{D_1}{Dt}\theta\right\} \tag{4.74}$$

C) Because our approach will be unfamiliar to most readers we will outline it briefly. We then go on to derive the main equation of this paper, the governing equation for the motion of the axis. The work here will not be done with broken line profiles as that introduces extra equations via the jump conditions, sources for numerical error, instead of simplifying the analyses as in Section 3. Our profile $v(\eta)$ will blend smoothly into the outside value $v = 0$ at $\eta = \pm 1$. We will take information from the jet region in the form of equation (4.72) integrated. One unknown term in there will be evaluated (in terms of the unknown axis position Y) by using information from the far regions I and III and the boundary conditions at ∞, with the aid of Green's formula. We will get a governing equation for Y, which will give future positions for given initial conditions.

If we take (4.72), put in (4.73) and (4.74), integrate $\int_{-1}^{1} d\eta$, note that all the terms in (4.73) and (4.74) are independent of η, recall h = 1 to $O(\lambda)$, recall $U = U_\eta = 0$ at $\eta = \pm 1$, and use the appropriate part of the continuity equation (4.53) and $\frac{D_1}{Dt}(U + a\mu_A) + a\nu_A \frac{D_1}{Dt}\Theta = 0$ at $\eta = \pm 1$, we get

$$\left(a\frac{\partial}{\partial t} + a\Psi\cos\Theta\frac{\partial}{\partial X}\right)\frac{\partial P}{\partial \eta}\Big|_{\Pi_b}^{\Pi_a} = \tag{4.75}$$

$$\Big\{a\cos\Theta\,\Theta_X\left(2a\frac{\partial}{\partial t} + (\langle U\rangle + 2a\Psi)\cos\Theta\frac{\partial}{\partial x}\right)(\dot{Y}\sin\Theta + \dot{\Psi})$$

$$- a\cos\Theta\frac{\partial}{\partial X}\left(2a\frac{\partial}{\partial t} + (\langle U\rangle + 2a\Psi)\cos\Theta\frac{\partial}{\partial X}\right)(-\dot{Y}\cos\Theta)$$

$$+ \left(\langle U^2\rangle\cos\Theta\frac{\partial}{\partial X} + \langle U\rangle\left(a\dot{Y}\sin\Theta + a\Psi + a\frac{\partial}{\partial t} + \cos\Theta\Psi_X + a\Psi\cos\Theta\frac{\partial}{\partial X}\right)\right.$$

$$\left. + 2\left(a\dot{Y}\sin\Theta + a\Psi\right)\left(a\frac{\partial}{\partial t} + \cos\Theta\Psi_X + a\Psi\cos\Theta\frac{\partial}{\partial X}\right)\right)\cos\Theta\,\Theta_X\Big\} = 0$$

For a known profile U (hence $\langle U\rangle$ and $\langle U^2\rangle$), and Ψ (which drops out in the linear problem we will do in this paper so it will not be discussed further here), once we express $\frac{\partial P}{\partial \eta}\Big|_{\Pi_b}^{\Pi_a}$ in terms of Y (or Θ) this becomes the sought-for governing equation for the axis motion. Let P_f be the far field pressure, that is, the pressure in regions I and III. We then have at $\eta = \pm 1$

$$P_f = P_A + \frac{m}{a}P_m \tag{4.76}$$

(plus a term on one $\overset{\text{side}}{\text{side}}$ constant in X and t resulting from the change in pressure associated with P_J. For the Gulf Stream this represents a change in surface height across the stream, and can be shown to play no other role than "maintaining" the stream, and so we drop it).

The smooth jet profile also supports no normal derivative jump,

$$\frac{\partial P_f}{\partial \eta} = \frac{m}{a}\frac{\partial P_m}{\partial \eta} \tag{4.77}$$

Now consider Figure 4.2. As discussed above we are after the large meandering behavior found in RLF. We will cut a section out of the stream to look at by taking p to be periodic in x in regions I and III. We will not need to go into the fuller boundary conditions, the inlet conditions which are discussed in RLF, in this paper. We let $p \to 0$ as $y \to \pm\infty$. Viewing this as the $z = x + iy$ plane we can transform region III to the $f = e^{-iz} = re^{i\phi}$ plane, with f single valued and analytic inside C. See Figure 4.3.

Here

$$r = e^{y}, \quad \phi = -x; \quad y = \ln r, \quad x = -\phi. \tag{4.78}$$

Region I would use $f = e^{iz}$, so

$$r = e^{-y}, \quad \phi = x; \quad -y = \ln r, \quad x = \phi \tag{4.79}$$

At some time step we know Y and $\dot{Y}$. RLF (p. 223) have

$$P_A(\eta, \bar{X}, t) = -\frac{1}{\lambda}\int_0^{\bar{X}} d\bar{x}\,\frac{h\nu_A(\bar{x},t)}{\cos\theta(\bar{x},t)} = \frac{1}{\lambda}\int_0^{\bar{X}} d\bar{x}\,(1+\lambda_1\kappa)\,\dot{Y}(\bar{x},t) \tag{4.80}$$

and so we know P_A. Hence we know P_f by (4.76), to $O(\lambda, m)$ along C, the transform of Y. If we can get $\partial P_f/\partial\eta$, then (4.77) will give . Then from (4.75) we can get $\ddot{Y}$, and time step forward to get a new Y and $\dot{Y}$, and repeat. To get $\partial P_f/\partial\eta$ we follow notationally as closely as possible the presentation given by Longuet-Higgins and Cokelet (1976;LC) for a very different problem, since we will use much of their numerical integration techniques in our subsequent paper.

See Figure 4.4. We will now exploit the structure of the equation $\nabla^2 P_f = 0$ in the far field. Define

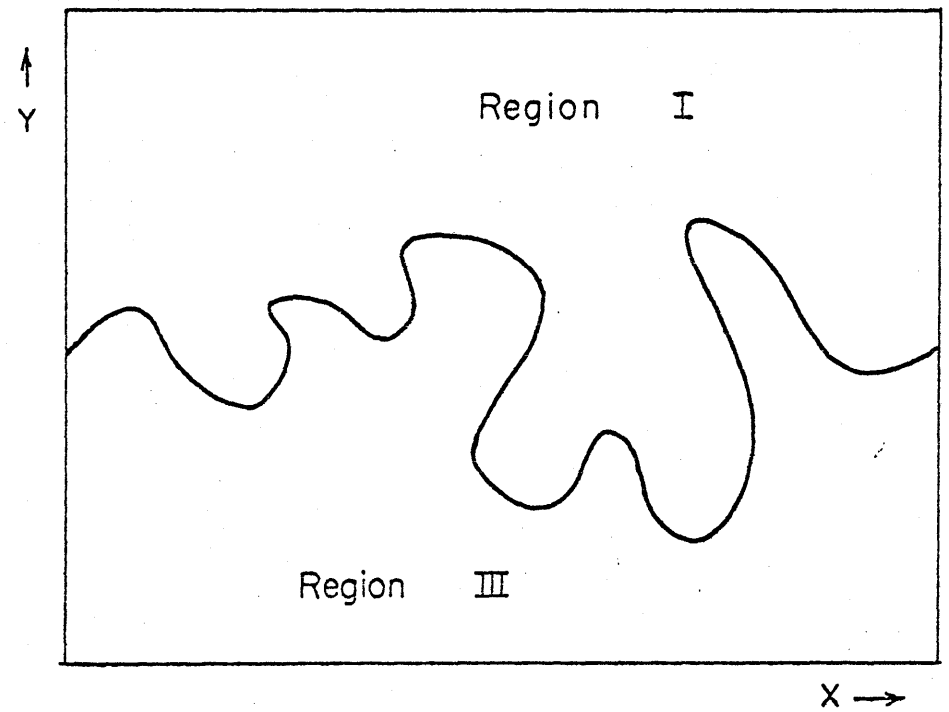

Figure 4.2

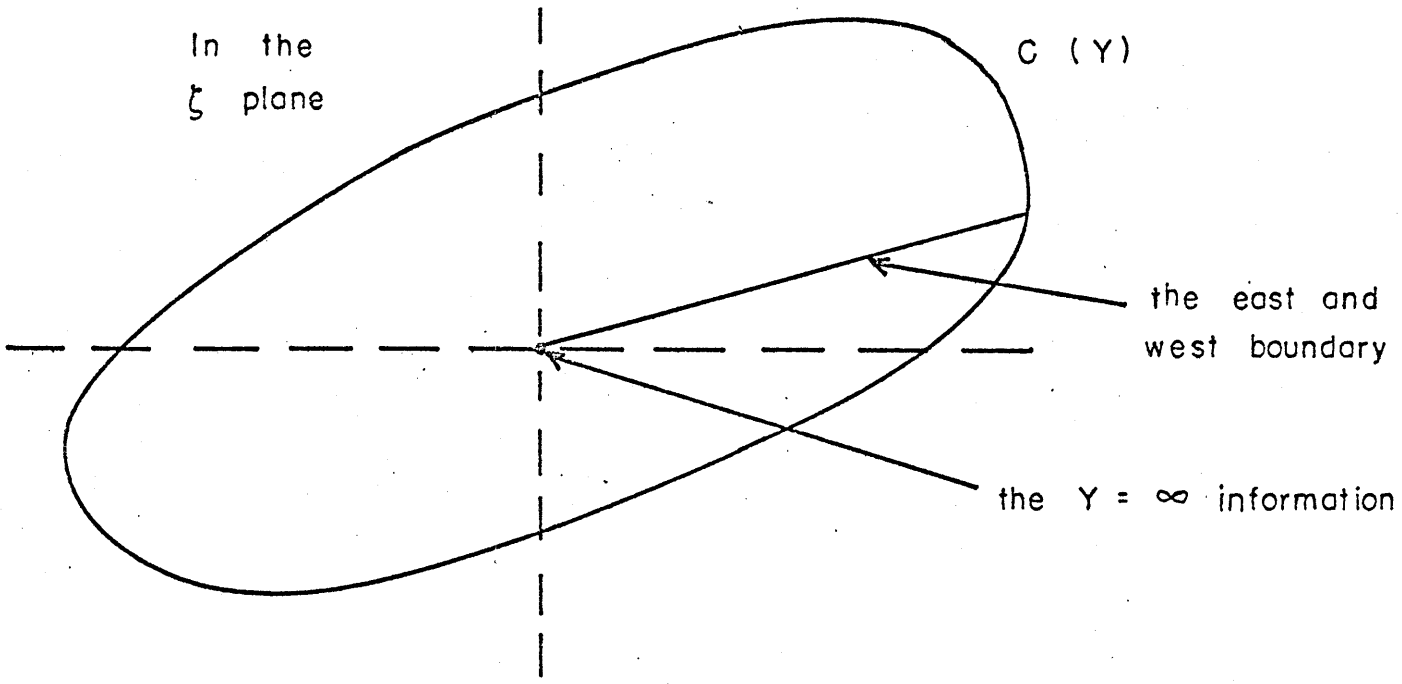
In the
ζ plane
C (Y)
the east and
west boundary
the Y = ∞ information

Figure 4.3

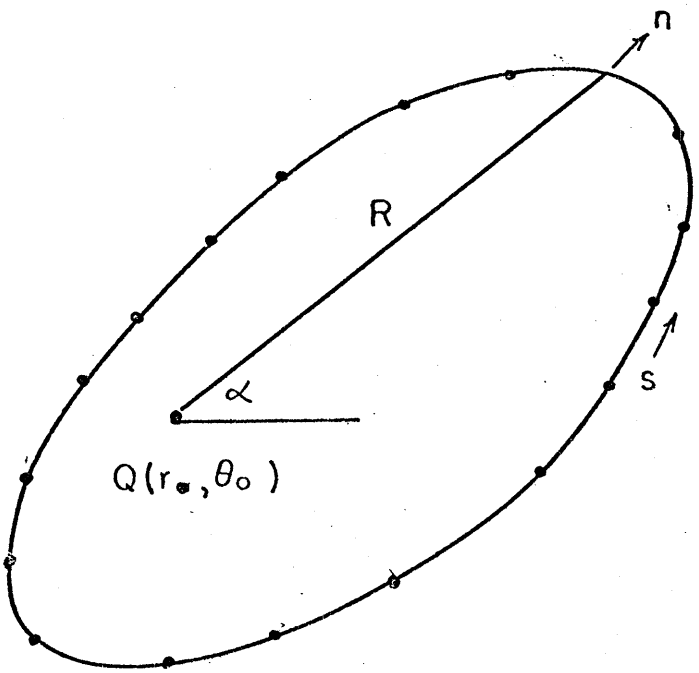

Figure 4.4, from LC

$$S' = \frac{1}{2\pi} \ln R \tag{4.81}$$

For a point such as $Q(r_0, \theta_0)$, we have

$$P(r_0, \theta_0) = \int_C \left(P \frac{\partial S'}{\partial n} - \frac{\partial P}{\partial n} S' \right) ds = \frac{1}{2\pi} \int_C \left(P \frac{\partial \alpha}{\partial s} - \frac{\partial P}{\partial n} \ln R \right) ds \tag{4.82}$$

In the limit that $Q(r_0, \theta_0) \to C$, we get

$$\int_C P \, d\alpha = \pi P_0 + \oint P \, d\alpha \tag{4.83}$$

and putting this into (4.80), and putting the known P_A into the right-hand side, we get

$$\int_C \frac{\partial P_f}{\partial n} \ln R \, ds = \oint_C P_A \, d\alpha - \pi P_A \tag{4.84}$$

This can be numerically solved as LC discuss. We thus have $\partial P_f / \partial n$ from which we can get $\partial P_f / \partial \eta$ and then by (4.77) the sought-for $\partial P_m / \partial \eta$. We must do this for both region I and region III.

We have now achieved our goal of making (4.75) an evolution equation for Y. Before plunging into numerics, we will look in the next section at the linear limit of the above to see how the method works in the simplest case.

5. The Full Nonlinear Problem in the Linear Limit

In the last section we achieved the primary goal of this paper, to derive a formula by which we could follow the evolution of the stream's axis to finite and large meanders. LC described the numerics for their less messy problem as very sensitive. We expect no less for our problem, and that will be the topic of a subsequent paper. Here we want to gain a little more understanding of our approach by looking at its analytically manageable linear limit. In subsection A we look at our method of integrating out region II. We can match (4.75) to the far field solutions directly in this linear limit. The resulting dispersion relation is very similar to that which we got from our top-hat model in Section 3. Thus, we gain support for this part of our method. In subsection B we go through the other distinct part of our method, Green's formula approach, which can be done analytically in the linear case. We regain the same dispersion relation as in subsection A, and hence support for this part of our method too.

A) Thinking of a perturbation like those discussed and drawn in Section 3, we linearize (4.75) in Θ and Ψ. We get

$$\left(a\frac{\partial}{\partial t}\right)\frac{\partial P_n}{\partial \eta}\Big|_{-1}^{+1} = 2a^2 Y_{tt\bar{x}} + 2a\langle U\rangle Y_{t\bar{x}\bar{x}} + \langle U^2\rangle Y_{\bar{x}\bar{x}\bar{x}} \qquad (5.1)$$

(4.80) can be approximated

$$P_n = \frac{1}{\lambda}\int_0^{\bar{z}} d\bar{x}\, \dot{Y}(\bar{x},t) \qquad (5.2)$$

The coordinates can also be written linearly $\bar{x} \to x$ and $\eta \to -y$. Plugging in the usual modal type solution $Y = Y_0 e^{in(x-ct)}$ for a linear problem, we have

$$P_A = -\frac{c}{\lambda} Y_0 e^{ik(x-ct)} \tag{5.3}$$

and, in particular, it has this value at $y = \pm 1$.

Now $(\partial^2/\partial y^2 + \lambda^2 \partial^2/\partial x^2) P_f = 0$ has as a solution, which can be matched to (5.3) according to (4.76) (to $O(\gamma_2)$),

$$P_f = P_0 e^{ik(x-ct)} e^{(\mp)\lambda k y} \tag{5.4}$$

in Region I (Region III), so (4.76) relates P_0 to Y_0 as

$$P_0 e^{ik(x-ct)} e^{(\mp)\lambda k} = -\frac{c}{\lambda} Y_0 e^{ik(x-ct)} \quad \text{at } y = (\mp) 1 \tag{5.5}$$

Now from (4.77), using (5.5) in the final step to substitute for p_0

$$\frac{\partial P_m}{\partial \eta} = \frac{a}{m} \frac{\partial P_f}{\partial \eta} = -\frac{a}{m} \frac{\partial P_f}{\partial y} \tag{5.6}$$

$$(\mp) \frac{a}{m} \lambda k P_0 e^{ik(x-ct)} e^{(\mp)\lambda k} = (\mp) \frac{a}{m} c k Y_0 e^{ik(x-ct)} \quad \text{at } y = (\mp) 1$$

Therefore,

$$\left(a \frac{\partial}{\partial t}\right) \frac{\partial P_m}{\partial \eta} \Big|_{-1}^{+1} = 2a \frac{\partial}{\partial t} \frac{\partial P_m}{\partial \eta} \Big|_{-1}^{+1} = -2 \frac{a^2}{m} c k Y_0 e^{ik(x-ct)} \tag{5.7}$$

Plugging this into (5.1) gives

$$\frac{2a^2c^2}{m} + 2a^2c^2k - 2ackc\langle v \rangle + k\langle v^2 \rangle = 0 \tag{5.8}$$

Consider now scales such as we see in the Gulf Stream, so $k \sim O(1)$. As discussed in Section 3 we can then let $\tanh \lambda k \to \lambda k$ in (3.12), giving

$$(1 - ac)^2 \lambda k = -(ac)^2 \tag{5.9}$$

If we now take a profile that fulfills the requirements on v of Section 4,

but approaches the top-hat profile (see Fig. 5.1), plug it into (5.8), and recall $\lambda = m$, we regain (5.9). As dispersion relations are the essence of such linear problems, we have shown the equivalence of the two approaches in this limit.

It is straightforward to include the β effect. We would get

$$\frac{2a^2c^2}{m}\sqrt{\beta_{ac}+k^2} + 2a^2k^2c^2 - 2ak^2c\langle U\rangle + k^2\langle U^2\rangle - \beta\langle U\rangle + 2ac\beta = 0 \tag{5.10}$$

which corresponds to (3.13)

B) Here we will start as in subsection A above. (5.1) holds, and we again get (5.3). But then we handle the far field differently. We go back to, to leading order,

$$P_f = P_A \tag{4.76}$$

We will look explicitly at Region III, and use the coordinate transformations to $f = re^{i\phi}$ space given in Section 4,

$$r = e^{\gamma}, \quad \phi = -x; \quad y = \ln r, \quad x = -\phi \tag{4.78}$$

to go to polar coordinates. The interface gets transformed into a circle

$$\mathcal{C}: r = e^{-\lambda k} \tag{5.11}$$

and the pressure on it becomes

$$P_A = -\frac{c}{\lambda}\gamma_0 e^{-ik\phi}e^{-ikct} \tag{5.12}$$

at $r = e^{-\lambda k}$. At the end of this section we will need to undo all these transforms according to

$$\frac{\partial P_f}{\partial \eta} = -\frac{\partial P_f}{\partial y} = -\frac{\partial P_f}{\partial r}\frac{\partial r}{\partial y} = \frac{\partial P_f}{\partial r}\lambda k e^{-\lambda k} \tag{5.13}$$

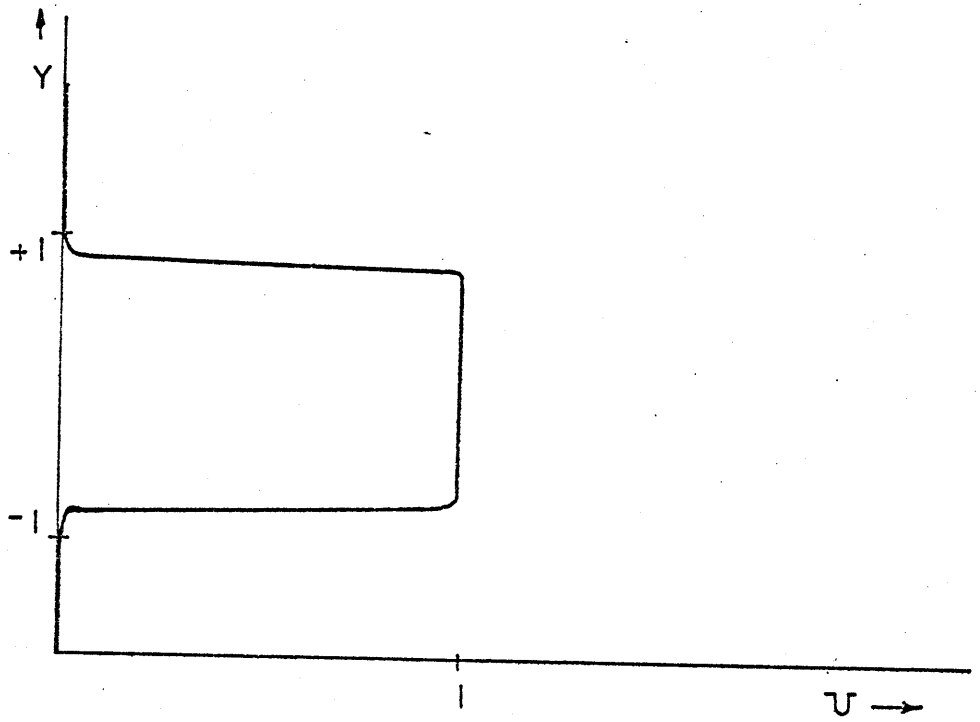

Figure 5.1

where the radial $\hat{r}$ corresponds here to $\hat{n}$ in equations (4.82)-(4.84). To get $\partial P_s/\partial r$ in (5.13) we will use

$$\int \frac{\partial P_s}{\partial r} \ln R \, ds = \oint P_A \, d\alpha - \pi P_A \tag{4.84}$$

First we consider the term $\oint P_A \, d\alpha$. We can parameterize the point traversing $\mathcal{C}$ which we call $\underline{s}$ by the central angle γ (see Fig. 5.2). With ϕ being the angle coordinate of any point in $\mathcal{S}$ space and labelling the angle of $\underline{p}$ by ϕ_0, we have

$$\gamma = \phi - \phi_0 \tag{5.14}$$

α is shown again as it was in Figure 4.4. With these (5.12) becomes

$$P_A = -\frac{c}{\lambda} Y_0 e^{-ikct} e^{-i\phi_0} e^{-i\gamma} \tag{5.15}$$

By elementary geometry

$$\gamma = 2\alpha \tag{5.16}$$

and then we explicitly get

$$\oint_{\mathcal{C}} P_A \, d\alpha = 0 \tag{5.17}$$

We are left with

$$\oint_{\mathcal{C}} \frac{\partial P_s}{\partial r} \ln R \, ds + \pi \left(-\frac{c}{\lambda} e^{-ikct} e^{-i\phi} \right) = 0 \tag{5.18}$$

We will briefly develop some general results to use to solve this. (5.18) is a Fredholm integral equation of the first kind with a singular kernel for the function $\partial P_s/\partial r$. We will call this function F for notational ease. Also, this helps to avoid confusing inward and outward normals, $\hat{n}_i$ and $\hat{n}_e$, in inner and outer domains, with $\hat{r}$, a coordinate in $\mathcal{S}$ space.

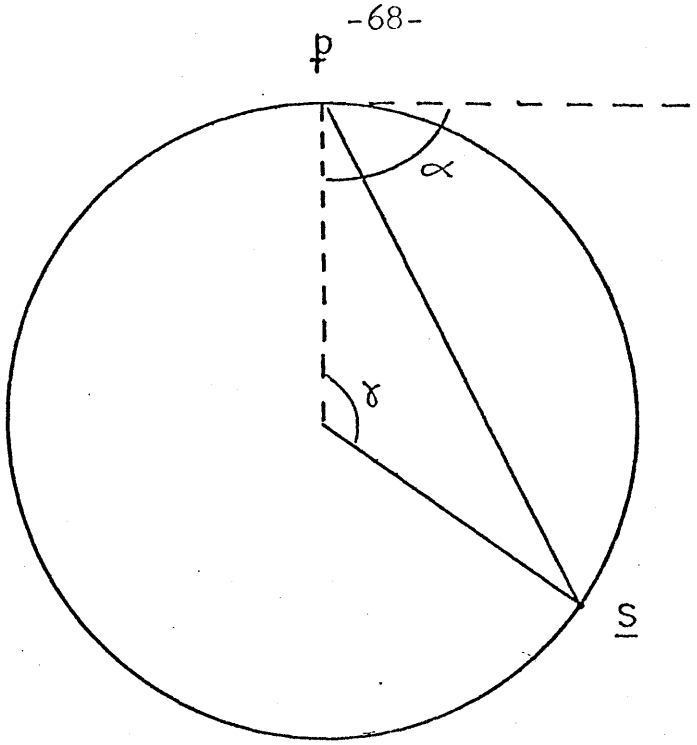

Figure 5.2

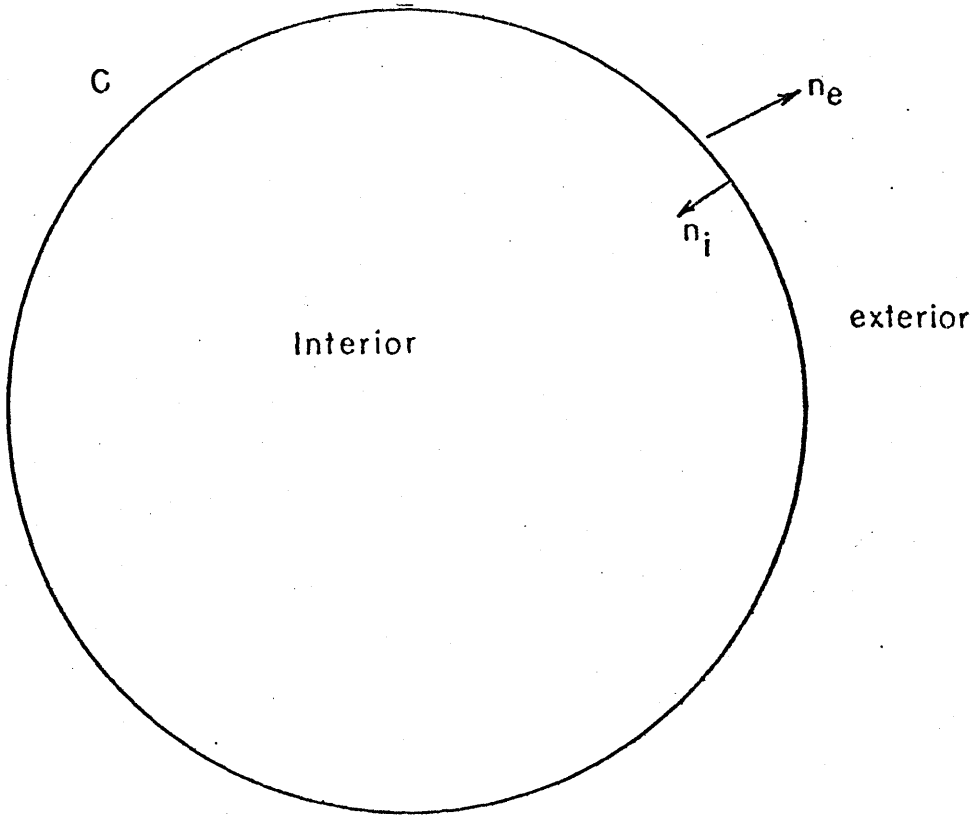

Figure 5.3

If a solution to an equation such as (5.19) exists, it generates the harmonic single-layer logarithmic potential (Symm, 1964)

$$V = V(\underline{P}) = \int_C F(\underline{s}) \ln |\underline{s} - \underline{P}| \, ds \qquad \underline{P} \in D + C \tag{5.19}$$

where D is either the interior domain $D = D_i$ (with associated $V \equiv V_i$) or the exterior domain $D = D_e$ (with associated $V \equiv V_e$) into which C divides the plane. As $\underline{P} \to C$ (when it is on C we will label it $\underline{p}$) V must be such that $V \to -\pi F_A$. There is only one harmonic on D_i that satisfies the given boundary conditions. On D_e there are infinitely many, which differ by their behavior at ∞. The solution defined by (5.19) behaves there as

$$V_e(\underline{P}) = c \ln P + O(1/P) \tag{5.20}$$

where $P = |\underline{P}|$ and $c = \int_C F(\underline{s}) \, ds$. This solution does not have the constant term which would dominate the $O(1/P)$ term. This becomes particularly important for s = 0, as we will have below, in which case $V_e \sim O(1/P)$.

Beginning with a point in the region of interest (interior or exterior; see Fig. 5.3), and one on C one can take the limit of the finite difference $\Delta V / |\Delta \underline{P}|$, where V on C can be evaluated by Plemejl's formula (Carrier, Krook, and Pearson, 1966, appendix) in this 2-D problem, though analogous results can be shown to hold in 3-D. One gets

$$\frac{\partial V_i}{\partial n_i}(\underline{p}) = \int_C F(\underline{s}) \frac{\partial}{\partial n_i} \ln |\underline{s} - \underline{p}| \, ds + \pi F(\underline{p}) \tag{5.21}$$

$$\frac{\partial V_e}{\partial n_e}(\underline{p}) = \int_C F(\underline{s}) \frac{\partial}{\partial n_e} \ln |\underline{s} - \underline{p}| \, ds - \pi F(\underline{p}) \tag{5.22}$$

where ∂_{ζ_n} acts at $\underline{p}$ on $\ln|\underline{s}-\underline{p}|$. Recalling

$$\hat{n}_i = -\hat{n}_e \quad \text{at } \underline{p} \tag{5.23}$$

we see

$$\frac{\partial}{\partial n_i}\ln|\underline{s}-\underline{p}| + \frac{\partial}{\partial n_e}\ln|\underline{s}-\underline{p}| = 0 \tag{5.24}$$

for $\underline{s} \neq \underline{p}$. Hence adding (5.21) and (5.22) gives

$$\frac{\partial V_i}{\partial n_i}(\underline{p}) + \frac{\partial V_e}{\partial n_e}(\underline{p}) = 2\pi F(\underline{p}) \tag{5.25}$$

Consider now the integral around a circle of radius a

$$\int_L G(s)\ln|\underline{s}-\underline{p}|\,ds = A\cos\beta \tag{5.26}$$

where $\underline{p}=(a,\beta)$, $\underline{s}=(a,\theta)$. We see a, and hence the unique, interior harmonic is

$$V_i(\underline{p}) = -\frac{A}{a}r\cos\theta \tag{5.27}$$

The exterior harmonic of the required type (5.19) is

$$V_e(\underline{p}) = Aa\frac{\cos\theta}{r} \tag{5.28}$$

By (5.25)

$$G(s) = \frac{1}{2\pi}\left(\frac{\partial V_i}{\partial n_i} + \frac{\partial V_e}{\partial n_e}\right) = -\frac{A}{\pi a}\cos\theta \tag{5.29}$$

This holds for any constant A, including if A is imaginary. We could do a similar proof for forcing $\sin\beta$.

But we now see that (5.26) is our equation (5.18) with

$$a \leftrightarrow e^{-\lambda k}, \quad F \leftrightarrow G, \quad \beta \leftrightarrow -\phi \text{ and } A \leftrightarrow -\frac{c\pi}{\lambda}e^{-ikct} \tag{5.30}$$

for the real part of $e^{-i\phi}$ and $A \leftrightarrow \frac{-i\epsilon\pi}{\lambda} e^{-ikct}$ for the imaginary part. We therefore get

$$\frac{\partial p_f}{\partial r} = -\frac{c}{\lambda} e^{-ikct} Y_0 e^{-i\phi} \frac{1}{e^{-\lambda k}} \tag{5.31}$$

Putting this into (5.13) then gives

$$\frac{\partial p_f}{\partial \eta} = \epsilon k Y_0 e^{-i\phi} e^{-ikct} \tag{5.32}$$

and then (4.77) becomes

$$\frac{\partial p_m}{\partial \eta} = \frac{a}{m} \frac{\partial p_f}{\partial \eta} = \frac{a\epsilon k}{m} Y_0 e^{ik(x-ct)} \tag{5.33}$$

which is (5.6) again.

A similar treatment for Region I gives the same results with a sign change. All subsequent steps leading to (5.8) then follow. We have verified the equivalence in the linear limit of the Green's formula method with the procedure of getting the needed information directly from the structure of the far field solution, as in Section 5A. And we have shown that either of these, when used with the integrate-across-the-stream approach, gives the same dispersion relation as the standard approach.

Appendix A The Vorticity Equation Frame for Section 2

The hydrostatic, Boussinesq, β plane (with $f = f_0 + \beta y$) thin-shell equations of motion are, with p the reduced dynamic pressure

$$\left(\frac{\partial}{\partial t} + u\frac{\partial}{\partial x} + v\frac{\partial}{\partial y} + w\frac{\partial}{\partial z}\right)u - fv = -p_x + \frac{\partial}{\partial z}\tau^{x,z} + \frac{\partial}{\partial x}\tau^{x,x} + \frac{\partial}{\partial y}\tau^{x,y} \qquad (A.1)$$

$$\left(\frac{\partial}{\partial t} + u\frac{\partial}{\partial x} + v\frac{\partial}{\partial y} + w\frac{\partial}{\partial z}\right)v + fu = -p_y + \frac{\partial}{\partial z}\tau^{y,z} + \frac{\partial}{\partial x}\tau^{y,x} + \frac{\partial}{\partial y}\tau^{y,y} \qquad (A.2)$$

$$0 = -p_z + b \qquad (A.3)$$

$$u_x + v_y + w_z = 0 \qquad (A.4)$$

$$\left(\frac{\partial}{\partial t} + u\frac{\partial}{\partial x} + v\frac{\partial}{\partial y} + w\frac{\partial}{\partial z}\right)b + N^2 w = 0 \qquad (A.5)$$

The depth of the water is H - h(x,y). All quantities in the above are dimensional.

We will nondimensionalize the above as follows. Let $u, v \sim U$, $x, y \sim L$, $t \sim T$, $z \sim H$, and $h \sim h_0$ where L, T, H, and h_0 are respectively a characteristic horizontal velocity, horizontal length, time, depth, and change in depth. We will scale $b \sim fUL/H$, though for the homogeneous fluid theories below $b \to 0$ which could be viewed as a rescaling. We will handle it by dropping (5) and making (3) $p_z = 0$ (or equivalently removing the b term from our vorticity equation below). We scale $p \sim fUL$ and $w \sim \delta(\frac{h_0}{H})U$ where the δ allows different

scalings of W. It is often taken $\delta = \varepsilon$, but we will leave it free for now. The theories that retain the lateral eddy viscosity parameterize τ as $\tau^{(x),(z)} = A_H \frac{\partial}{\partial(y)}\begin{pmatrix} u \\ v \end{pmatrix}$ so we will scale it $\tau^{(x),(y)} \sim \frac{A_H U}{L}$. The problem with these lateral terms is that we have equally poor estimates of the scale of A_H and of the stresses themselves. In the vertical we have some additional information. We know roughly what the stress at the free surface is (labeled $\tilde{\tau}^{(x)}$ hereafter) and we can use that for a scale. It would take us too far astray here to go into the theory of Ekman boundary layers. Pedlosky (1979, p.74) gives a very clear presentation and we will appropriate results when needed. Here we want to indicate the effects of these boundary layers on our scaling. If the nondimensional orm of the surface stress, given below, affected the full water column, these terms would be negligible compared to other terms. This is not acceptable, since the stress at the free surface is driving the system, so to ignore it is clearly to ignore crucial information. The nondimensional term becomes larger and larger as one thinks of the effects being restricted to a shallower and shallower depth. We will introduce a depth H', the boundary layer depth, over which the stress effects are directly felt and with which the stress term in the equation becomes comparable to the other terms. The no-slip condition at the bottom sets up a bottom stress and so an analysis layer is formed there. Unlike the top layer, the bottom stress is not an imposed parameter but rather results from the solution flow itself. As mentioned above, we will simply use the results of Ekman layer theory here.

We will introduce the nondimensional parameters

$$\varepsilon = \frac{U}{f_0 L} \qquad \epsilon = \frac{1}{f_0 T} \qquad \hat{\beta} = \frac{\beta L}{f_0} \qquad S = \frac{h_0}{H} \qquad S(z) = \frac{N^2(z) H^2}{f_0 L^2} \qquad \alpha = \frac{A_H}{L^2 f_0}$$

and a measure of the vertical viscosity effects, γ. Outside the boundary layers we would define $\gamma = \frac{\tau_0}{H'U}$ or $A_V/H^2 f$ and with oceanic values the γ term is negligible. However, in the top boundary layer, $\gamma_T = \frac{\tau_0}{H'U} = 10^{-3}$ is comparable to other terms. We will talk about the scaling in the bottom boundary layer below. For the moment we will just carry it all as γ though the term has different scales in different places.

With the variables and functions now nondimensional we get

$$\varepsilon\left(\frac{\epsilon}{\varepsilon}\frac{\partial}{\partial t} + u\frac{\partial}{\partial x} + v\frac{\partial}{\partial y} + \delta w\frac{\partial}{\partial z}\right)u - (1+\hat{\beta}y)v = -P_x + \gamma\frac{\partial}{\partial z}\tau^{x,z} + \alpha\left(\frac{\partial}{\partial x}\tau^{x,x} + \frac{\partial}{\partial y}\tau^{x,y}\right) \quad \text{(A.6)}$$

$$\varepsilon\left(\frac{\epsilon}{\varepsilon}\frac{\partial}{\partial t} + u\frac{\partial}{\partial x} + v\frac{\partial}{\partial y} + \delta w\frac{\partial}{\partial z}\right)v + (1+\hat{\beta}y)u = -P_y + \gamma\frac{\partial}{\partial z}\tau^{y,z} + \alpha\left(\frac{\partial}{\partial x}\tau^{y,x} + \frac{\partial}{\partial y}\tau^{y,y}\right) \quad \text{(A.7)}$$

$$0 = -P_z + b \quad \text{(A.8)}$$

$$u_x + v_y + \delta w_z = 0 \quad \text{(A.9)}$$

$$\varepsilon\left(\frac{\epsilon}{\varepsilon}\frac{\partial}{\partial t} + u\frac{\partial}{\partial x} + v\frac{\partial}{\partial y} + \delta w\frac{\partial}{\partial z}\right)b + \Delta'\delta w = 0 \quad \text{(A.10)}$$

We would like to eliminate the $\delta w\frac{\partial}{\partial z}$ terms here. For a stratified ocean equation (10), for $\Delta' \sim O(1)$ as in the ocean, requires at most $\delta \sim \varepsilon$ and so we can drop it from the advective derivative. For a homogeneous ocean ($b \equiv 0$) away from boundary layers, where ε, γ, and α, terms can all be ignored, differentiating (A.6) and (A.7) with respect to z and using (A.8) gives $u_z = v_z = 0$ to leading order, so we can

drop $\delta w \frac{\partial}{\partial z}$. In the Ekman layers, where the dimensional dominant balance of the deviation from geostrophy is $f\begin{pmatrix} -v \\ u \end{pmatrix} = \frac{\partial}{\partial z}\tau^{(x)}_{(y),z}$ we get $-f w_z = \frac{\partial}{\partial z}\hat{k}\cdot \mathrm{curl}\,\vec{\tau}$. Boundary layers are where O(1) changes occur over short distances, so $w_z \sim \delta(H/L)(U/H)$. Integrating over the boundary layer, the scales are $f\,\delta(H/L)U = \tau_0/L$ or $\delta = \tau_0/fHU \sim (1\ \mathrm{cm^2/sec^2})/(10^{-4}\ 1/\mathrm{sec})(5\times10^5\ \mathrm{cm})(1\ \mathrm{cm/sec}) = 2\times10^{-2}$ in the open ocean Ekman layer. So we can drop the $\delta w \frac{\partial}{\partial z}$ here too. (And here too we can, from (A.9), say $u_x + v_y = 0$ to leading order, which of course $\Leftrightarrow$ the nondimensional $w_z = 0$ to any order.) We now drop it over our domain and will not belabor it further.

Adding $\frac{\partial}{\partial x}$(A.7) to $-\frac{\partial}{\partial y}$(A.6) we get

$$\varepsilon\left(\frac{\varepsilon}{\varepsilon}\frac{\partial}{\partial t} + u\frac{\partial}{\partial x} + v\frac{\partial}{\partial y}\right)(v_x - u_y) + \varepsilon(u_x v_x + v_x v_y - u_y u_x - v_y u_y)$$
$$+\hat{\beta}v + (1+\hat{\beta}y)(u_x + v_y) = \gamma\frac{\partial}{\partial z}\left(\tau^{y,z}_x - \tau^{x,z}_y\right) + \alpha\left(-u_{yyy} - u_{xxy} + v_{xxx} + v_{yyx}\right) \qquad \text{(A.11)}$$

Provided $\hat{\beta}, \varepsilon << 1$ we can make two simplifications. Open ocean values are $\hat{\beta} = (10^{-13}\ 1/\mathrm{cm\text{-}sec})(10^8\ \mathrm{cm})/(10^{-4}\ 1/\mathrm{sec}) = .1$ and $\varepsilon = (1\ \mathrm{cm/sec})/(10^{-4}\ 1/\mathrm{sec})(10^8\ \mathrm{cm}) = 10^{-4}$, and even in the oceanic jets with $U \sim 30$ cm/sec and $L \sim 50$ km these will be $<< 1$. Therefore

$$(1+\hat{\beta}y)(u_x + v_y) \approx (u_x + v_y) = -\delta w_z$$

and also

$$\varepsilon(u_x v_x + v_x v_y - u_y u_x - v_y u_y) = \varepsilon(u_x + v_y)(v_x - u_y) = -\varepsilon\delta(v_x - u_y)w_z$$
$$<< \delta w_z$$

and so it can be dropped. Our vorticity equation (A.11) is now

$$\varepsilon\left(\frac{\varepsilon}{\varepsilon}\frac{\partial}{\partial t} + u\frac{\partial}{\partial x} + v\frac{\partial}{\partial y}\right)\left(v_x - u_y + \frac{\hat{\beta}}{\varepsilon}y\right) - \delta w_z = \gamma\frac{\partial}{\partial z}\left(\tau^{y,z}_x - \tau^{x,z}_y\right) \qquad \text{(A.12)}$$
$$+\alpha\left(-u_{yyy} - u_{xxy} + v_{xxx} + v_{yyx}\right)$$

Here we should delineate two cases. The first is a homogeneous ocean, and in this case there are two ways to think of things. We can deal with the ocean as viscous even though the direct effects occur only in thin boundary layers. Then we integrate the equations from top to bottom, and apply the stress conditions at the top (wind) and bottom (unknown, but can be determined as part of the solution). The W_{Top} is taken as negligible for scales we are looking at, while $W_B = \frac{S}{\delta}\vec{V}_B \cdot \nabla h$. The other approach is to deal with the boundary layers separately and see what W the Ekman layers give for given stress (top) and interior flow (bottom). Then we integrate over the interior, treating it as inviscid and use the Ekman W for W_T, and for W_B we use the Ekman W there plus the inviscid slope, $W_B = W_{EB} + \frac{S}{\delta}\vec{V}\cdot\nabla h$. It turns out, not surprisingly, that $W_T = \gamma_T(\tilde{\tau}_x - \tilde{\tau}_y)$, so the wind effects come back in as they must. In fact, we see that the top conditions are the same either way. $W_B = \frac{S}{\delta}\vec{V}\cdot\nabla h + \frac{1}{2}\sqrt{\frac{2A_v}{f_0}}(v_x - u_y)$, where we will now call $\frac{1}{2}\sqrt{\frac{2A_v}{f_0}} = R/\delta$. From either approach the result is

$$\varepsilon\left(\frac{\epsilon}{\varepsilon}\frac{\partial}{\partial t} + u\frac{\partial}{\partial x} + v\frac{\partial}{\partial y}\right)\left(v_x - u_y + \frac{\beta}{\varepsilon}y\right) - \gamma_T\left(\tilde{\tau}_x^y - \tilde{\tau}_y^x\right) + S\vec{V}\cdot\nabla h + R(u_x - v_y) \qquad (A.13)$$
$$= \alpha\left(-u_{yyy} - u_{xxy} + v_{yyx} + v_{xxx}\right)$$

or, quasigeostrophically,

$$\varepsilon\left(\frac{\epsilon}{\varepsilon}\frac{\partial}{\partial t} - P_y\frac{\partial}{\partial x} + P_x\frac{\partial}{\partial y}\right)\left(\nabla^2 P + \frac{\beta}{\varepsilon}y + \frac{S}{\varepsilon}h\right) - \gamma_T\left(\tilde{\tau}_x^y - \tilde{\tau}_y^x\right) + R\nabla^2 P = \alpha\nabla^4 P \qquad (A.14)$$

where

$$\nabla^4 = \frac{\partial^4}{\partial x^4} + 2\frac{\partial^4}{\partial x^2 \partial y^2} + \frac{\partial^4}{\partial y^4}$$

The second case is the stratified case. Here we can rewrite (A.10) as $\delta w = \frac{\epsilon}{\sigma}\left(\frac{\epsilon}{\varepsilon}\frac{\partial}{\partial t} + u\frac{\partial}{\partial x} + v\frac{\partial}{\partial y}\right)b$ and differentiate both sides by z. If we notice that $u_z b_x + v_z b_y$ (to lowest order) $= (-P_y)_z b_x + (P_x)_z b_y$

$= -b_y b_x + b_x b_y = 0$ we can write

$\delta w_z = \varepsilon \left(\frac{\epsilon}{\tau}\frac{\partial}{\partial t} + u\frac{\partial}{\partial x} + v\frac{\partial}{\partial y}\right)\frac{\partial}{\partial z}\frac{b}{s}$ and hence a vorticity equation

$$\varepsilon\left(\frac{\epsilon}{\tau}\frac{\partial}{\partial t} + u\frac{\partial}{\partial x} + v\frac{\partial}{\partial y}\right)\left(v_x - u_y + \frac{\partial}{\partial z}\frac{b}{s} + \frac{\hat{\beta}}{\varepsilon}y\right) = \alpha\frac{\partial}{\partial z}\left(\tau_x^{yz} - \tau_y^{xz}\right) \tag{A.15}$$

or, quasigeostrophically, $+\alpha(-u_{yyy} - u_{xxy} + v_{xxx} + v_{xyy})$

$$\varepsilon\left(\frac{\epsilon}{\tau}\frac{\partial}{\partial t} - p_y\frac{\partial}{\partial x} + p_x\frac{\partial}{\partial y}\right)\left(\nabla^2 p + \frac{\partial}{\partial z}\frac{p_z}{s} + \frac{\hat{\beta}}{\varepsilon}y\right) = \alpha\frac{\partial}{\partial z}\left(\tau_x^{yz} - \tau_y^{xz}\right) + \alpha\nabla^4 p \tag{A.16}$$

Appendix B The Pressure Jump Conditions

Our model which we develop in Section 3 will have much of its dynamics contained in the jump conditions on the perturbation pressure and its derivatives. Here we want to discuss at greater length than is common in the literature the derivation of these jump conditions. In particular, we want to show that there are two distinct ways of looking at them, physically and mathematically, discussing both.

We will picture a surface separating two flow regimes as in Figure B.1. Region 2 has a zonal background flow of $U(y)$, so $u^T = U + u^{(2)}$ there. The "T" superscript will denote "total," while the bracketed number appears on the perturbation flow and indicates the given region. In region 1 $u^T = u^{(1)}$. By the "linear case" we refer to infinitesimal displacements of an originally zonal interface and hence infinitesimal perturbation quantities $u^{(i)}$, $v^{(i)}$, and $p^{(i)}$.

We will here deal with a fluid whose motion in nondimensional variables is governed by (with derivations as in Appendix A)

$$\varepsilon \frac{D}{Dt} u - v = -p_x \tag{B.1}$$

where $D/Dt = \partial/\partial t + u\,\partial/\partial x + v\,\partial/\partial y$ and $\varepsilon = U_0/f_0 L$

$$\varepsilon \frac{D}{Dt} v + u = -p_y \tag{B.2}$$

$$u_x + v_y = 0 \tag{B.3}$$

where until further notice all functions carry an implied "T". When we talk about linearizing below we will imply an infinitesimal scale a, where

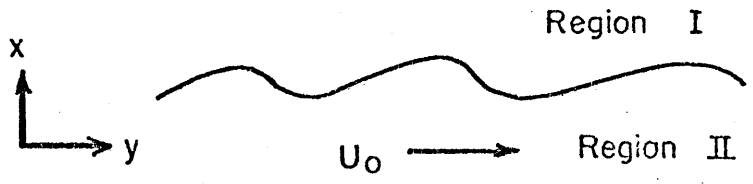

Figure B.1

$u^T = U + au$, $v^T = av$ and $p^T = \bar{P} + ap = -\int^y U + ap$

(the latter from the $O(a^0)$ terms in 3.2) but we will not explicitly carry it since its effects are clear as far as we will go.

From (B.3) we can define a streamfunction Ψ such that $-\Psi_y = u$, $\Psi_x = v$, but then we see from (B.1) and (B.2) that to $O(\epsilon)$ $\nabla\Psi = \nabla p$ so we will use p as the streamfunction. If we add $-\frac{\partial}{\partial y}$(B.1) to $+\frac{\partial}{\partial x}$(B.2) we get (B.4) $\epsilon\frac{D}{Dt}(v_x - u_y) = 0$ or to lowest order in ϵ, $\frac{D}{Dt}(\nabla^2 p^T) = 0$ (B.5)

Now we can follow two approaches. We can argue that we have a mathematical equation governing the motion which must hold for the full domain including the interface. In this approach, noting that our background flow has a step function discontinuity we expect our equation to have step functions, δ functions, δ' functions and so on. Such "functions" are of course limits of continuous functions and can be dealt with thusly when necessary. We posit the existence of a fluid surface that we will integrate the vorticity equation, with its above-mentioned singular functions, across to generate our matching conditions. This procedure includes the following two ideas. First, as to fluid moves, the usual arguments (Lamb, 1957), Yih (1965) give that a particle on the fluid surface should stay there. Second, the vorticity equation (B.4) or (B.5) says that all particles should maintain their vorticity. So if we start the process with a purely zonal interface the vorticity of particles on it then is $U_o\,\delta(y - \zeta(x))$, where we have labelled the interface by $y = \zeta(x)$, and that becomes their vorticity forever.

For the other approach we will invoke two physical ideas. First, the normal velocities on both sides of the interface must match for it to be a fluid surface. Second, total pressure must match to avoid infinite accelerations. We will see that these lead to the same matching conditions

as the mathematical approach and we will further see the interesting result that the two matching conditions become in a sense, for this quasigeostrophic case, different order conditions, something which is not usually brought out.

We will deal with the physical approach first. Let $F = y - \zeta(x,t) = 0$ define the fluid surface. The statement that a fluid particle on the surface stays there is the same as requiring the normal velocity of the surface match that of the fluid immediately on both sides of it and hence requiring that those velocities match each other. It can be written

$$\frac{D}{Dt} F = 0 = \zeta_t + u\zeta_x - v \tag{B.6}$$

Since the problem is linear and the coefficients are independent of x and t we can look at "modes," that is, Fourier components in x and t, one at a time. With the dependence $e^{ik(x-ct)}$ we can write (B.6) as

$$\zeta = \frac{v}{ik(U-c)} = \frac{p_x}{ik(U-c)} = \frac{p}{U-c}$$

With Δ an infinitesimal quantity, and $U(\zeta+\Delta) = U$ and $U(\zeta-\Delta) = U_0$ we then get the familiar linear condition $\frac{p^{(1)}|_{y=\zeta}}{-c} = \zeta = \frac{p^{(2)}|_{y=\zeta}}{U_0 - c}$ or

$$\left[\frac{p}{U-c}\right] = 0 \tag{B.7}$$

where $[X] = X|_{y=\zeta+\Delta} - X|_{y=\zeta-\Delta}$ *

---

*Besides the usual modal solutions, discrete points in $k-c$ space, which we will find, there exist for real c's the continuous solution (see Case, 1960), but these can be shown to be asymptotically unimportant. Hence, we restrict our attention to complex c's, and this all holds as stated for us without worrying about singularities in the limiting process that we glossed over.

The equation this result came from is an $O(\varepsilon^0)$ equation and in that sense this can be called a zeroth order boundary condition.

We now require continuity of pressure at the interface to avoid infinite accelerations. This guarantees $[\hat{t}\cdot\nabla P_T]=0$ where $\hat{t}$ is the tangent vector $\hat{t}=(1+(\zeta_x)^2)^{-1/2}(1,\zeta_x)$. Plugging in for ∇p into (B.2) and (B.1) gives

$$-\varepsilon\frac{D}{Dt}(U+u)+v-U\zeta_x-u\zeta_x-\zeta x\varepsilon\frac{D}{Dt}v=(1+(\zeta_x)^2)^{1/2}\hat{t}\cdot\nabla p \qquad (B.8)$$

Subtracting the value of this at $\zeta-\Delta$ from that at $\zeta+\Delta$, using $[\hat{t}\cdot\nabla p]=0$ and noting that $[\zeta_t]=0$ so (B.6) gives $[(U+u)\zeta_x-v]=0$, we get $\left[\frac{D}{Dt}(U+u)-\zeta_x\frac{D}{Dt}v\right]=0$ which linearizes to the familiar

$$\left[\left(\frac{\partial}{\partial t}+U\frac{\partial}{\partial x}\right)u+vU_y\right]=0=\left[(U-c)p_y-pU_y\right] \qquad (B.9)$$

We have seen this come out of the $O(\varepsilon)$ terms in the equations, and in that sense it is an $O(\varepsilon)$ matching condition.

Now let us look at the mathematical approach. We have $\frac{D}{Dt}(\nabla^2 P_T)=\left(\frac{\partial}{\partial t}+(U+u)\frac{\partial}{\partial x}+v\frac{\partial}{\partial y}\right)(\nabla^2 p-U_{yy})=0$ which linearizes to

$$\left(\frac{\partial}{\partial t}+U\frac{\partial}{\partial x}\right)\nabla^2 p-vU_{yy}=0 \qquad (B.10)$$

We could introduce a transition to take U smoothly from U_∞ to 0 to make everything well defined, but let us avoid that, it is not needed here, and use singular functions. U_{yy} is a δ' function at the interface, and for the equation to be zero everywhere including there some other term must become as singular. By inspection we see that if p is a step function, two terms are products of step functions and δ' functions. We can rewirte (B.10) as

$$\frac{\partial}{\partial y}\left(\left(\frac{\partial}{\partial t}+U\frac{\partial}{\partial x}\right)p_y-p_xU_y\right)+\left(\frac{\partial}{\partial t}+U\frac{\partial}{\partial x}\right)p_{xx}=0 \qquad (B.11)$$

where the most singular terms are now all in the first term. We will integrate $\int_{\beta-\Delta}^{\beta+\Delta} dy$. Note the second terms gives a negligibly small ($O(\Delta)$ and $\Delta \to 0$)contribution,and so we get, applying our modal condition

$$\left[\left(\frac{\partial}{\partial t} + U\frac{\partial}{\partial x}\right)P_y - P_x U_y\right] = 0 = \left[(U-c)P_y - P U_y\right] \qquad \text{(B.12)}$$

We have integrated the vorticity equation, which we know is an equation whose terms come from terms that were order ε in the original governing equations, over some sharp discontinuity to get the matching condition. It is not too surprising that the result is what we saw above came from order ε information in that approach.

Since 3.8 gives the jump to be zero and the functions are all continuous away from $y = \beta(x)$, we can write

$$(U-c)P_y - P U_y = (U-c)^2 \frac{\partial}{\partial y}\left(\frac{P}{U-c}\right) \equiv Q(y) \qquad \text{(B.13)}$$

where Q(y) is continuous. We integrate $\int_{\beta-\Delta}^{\beta+\Delta} (B.13)\, dy$, (note the right-hand side is negligible to $O(\Delta)$), and make an $O(\Delta)$ change in the rest by changing the integrand to $(U_0 - c)\frac{\partial}{\partial y}\left(\frac{P}{U-c}\right)$. This gives us

$$\left[\frac{P}{U-c}\right] = 0 \qquad \text{(B.14)}$$

So the second integration of the vorticity equation has given us what we before spoke of as the $O(\varepsilon^0)$ equation. Since the vorticity equation itself results from the differentiation of the momentum equations which are dominated by $O(1)$ balances in such a way that the higher terms cancel and reveal the $O(\varepsilon)$ terms it is not too surprising that integration can take us back to the $O(\varepsilon^0)$ level.

ACKNOWLEDGEMENTS

Primary thanks go to Dr. Glenn Flierl for suggesting this fascinating topic, and then following me through the intellectual meanders always involved in a student's first such project. Discussions with Drs. Joseph Pedlosky and James Luyten in the final period of this work were very helpful, particularly in calling to my attention certain aspects and implications of the model that I had not before thought about. The typing and editing by Joel Sloman and the figure drafting by Isabelle Kole, both tasks beyond my abilities, are greatly appreciated.

REFERENCES
(with author abbreviations used in the text)

Bolin, B. (1950). On the influence of the earth's orography on the westerlies. Tellus, 2, 184-195.

Bryan, K., Manabe, S., Pacanowski, R. (1975). A global ocean-atmosphere climate model. Part II. The oceanic circulation. J. Phys. Oc., 5, 30-46.

Carrier, G., Krook, M., Pearson, C. (1966). Functions of a Complex Variable. McGraw-Hill, N.Y.

Carrier, G., Robinson, A. (1962). On the theory of wind-driven ocean circulation. J. Fluid Mech., 12, 49-80.

Case, K. (1960). Stability of inviscid plane Couette flow. Phys. of Fluids, 3, 143-154.

Charney, J. (1955). The Gulf Stream as an inertial boundary layer. Proc. Nat. Acad. Sci., 41, 731-740.

Charney, J., Eliassen, A. (1949). A numerical method for predicting the perturbations of the middle latitude westerlies. Tellus, 1, 38-54.

Drazin, P.,Howard, L. (1966). Hydrodynamic stability of parallel flow of inviscid fluid, in Advances in Applied Mechanics, Vol. 9. Acad. Pr., N.Y.

Flierl, G., Robinson, A. (to be published; FR).

Flierl, G. (1976). Gulf Stream meandering, ring formation and ring propagation. Ph.D. Thesis, Harvard U.

Fofonoff, N. (1954). Steady flow in a frictionless homogeneous ocean. J. Mar. Res., 13, 254-262.

Fuglister, F., Voorhis, A. (1965). A new method of tracking the Gulf Stream. Limn. and Oc., Supp. to Vol. X, R115-R125.

Fukuoka, J. (1957). On the Tsushima Current. Jour. Oc. Soc. Jap., 13(2).

Golan, D. (1979). An experiment in large-scale air-sea interaction. S.M. Thesis, M.I.T.

Goldstein, S. (1938). Modern Developments in Fluid Mechanics, Vol. 1, Oxford U. Press.

Hansen, D. (1970). Gulf Stream meanders between Cape Hatteras and the Grand Banks. Deep-Sea Res., 17, 495-511.

Haurwitz, B., Panofsky, H. (1950). Stability and meandering of the Gulf Stream. Trans. Amer. Geo. Union, 31, 723-731.

Hildebrand, F. (1962). Advanced Calculus for Applications, Chapt. 7, Prentice-Hall, Inc., Englewood Cliffs, N.J.

Haidvogel, D., Holland, W. (1978). The stability of ocean currents in eddy-resolving general circulation models. J. Phys. Oc., 8, 393-413.

Holland, W. (1978). The role of mesoscale eddies in the general circulation of the ocean--numerical experiments using a wind-driven quasi-geostrophic model. J. Phys. Oc., 8, 365-392.

Kamenkovitch, V., Reznick, G. (1972). A contribution to the theory of stationary wind-driven currents in a two layer liquid. Isv., Atmos. and Oc. Phys., 8, 419-434.

Lamb, H. (1945). Hydrodynamics, Sixth Ed., Dover Publications, N.Y.

Lipps, F. (1963). Stability of jets in a divergent barotropic fluid. Jour. Atmos. Sci., 20, 120-129.

Longuet-Higgins, M., Cokelet,E. (1976; LC). The deformation of steep surface waves on water. I. A numerical method of computation. Proc. Roy. Soc. Lond. A, 350, 1-26.

Luyten, J. (1977). Scales of motion in the deep Gulf Stream and across the Continental Rise. J. Mar. Res., 35, 49-74.

Morgan, G. (1956). On the wind-driven ocean circulation. Tellus, 8, 301-320.

Munk, W. (1950). On the wind-driven ocean circulation. J. Met., 7, 79-93.

Munk, W., Carrier, G. (1950). The wind-driven circulation in ocean basins of various shapes. Tellus, 2, 158-167.

Parson, A. (1969). A two-layer model of Gulf Stream separation. J. Fluid Mech., 39, 511-528.

Pedlosky, J. (1979a). Seminar at Woods Hole on finite amplitude instabilities.

Pedlosky, J. (1979b). Geophysical Fluid Dynamics. Springer Verlag New York, Inc.,N.Y.

Rayleigh, Baron (1945). The Theory of Sound. Dover Publications, N.Y.

Robinson, A. (1963). Wind-Driven Ocean Circulation. Blaisdall Pub. Co.

Robinson, A. (1971). The Gulf Stream. Phil. Trans. Roy. Soc. A, 270, 551.

Robinson, A., Luyten, J., Flierl, G. (1975; RLF). On the theory of thin rotating jets: a quasi-geostrophic time dependent model. Geo. Fl. Dyn., 6, 211-244.

Robins, A., Niiler, P. (1967; RN). The theory of free inertial currents, I: path and structure. Tellus, 19, 269-291.

Rossby, C. (1940). Planetary flow patterns in the atmosphere. Quart. J. Roy. Met. Soc., 66, Supp., 66-87.

Schmitz, W., Robinson, A., Fuglister, F. (1970). Bottom velocity observations directly under the Gulf Stream. Science, 170, 1192-1194.

Stern, M. (1961). The stability of thermocline jets. Tellus, 13, 503-508.

Stommel, H. (1948). The westward intensification of wind-driven ocean currents. Trans. Am. Geo. Un., 29. 202-206.

Stommel, H. (1955). Discussion at the Woods Hole Convocation, June, 1954. J. Mar. Res., 14, 504-510.

Stommel, H. (1976). The Gulf Stream. California Libraries Reprint Series Edition, U. Cal. Press.

Symm, G. (1964). Integral Equation Methods in Elastic and Potential Theory. National Physics Lab., Math. Division (Teddington).

Sverdrup, H. (1947). Wind-driven currents in a baroclinic ocean; with application to the equatorial currents of the eastern Pacific. Proc. Nat. Acad. Sci., 33, 318-326.

Taft, B., Robinson, A., Schmitz, W. (1973). Current path and bottom velocities of the Kuroshio. J. Phys. Oc., 3, 347-350.

Takano, K. (1975). A numerical simulation of the world ocean circulation. Preliminary results, in Numerical Models of Ocean Circulation, Acad. of Sci., Washington, D.C.

Veronis, G. (1973). Model of world ocean circulation: I. J. Mar. Res., 31, 228-288.

Warren, B. (1963). Topographic influences on the path of the Gulf Stream. Tellus, 15, 167-183.

Yih, C. (1969). Fluid Mechanics. McGraw-Hill, Inc.